5

Rapid #: -2890689

Ariel IP: 128.59.152.191

Status	Rapid Code	Branch Name	Start Date
New	ZCU	Butler	10/22/2009 7:27:13 PM
Pending	ALM	Main Library	10/22/2009 7:27:22 PM
Batch Not Printed	ALM	Main Library	10/23/2009 8:01:42 AM
Unfilled	ALM	Main Library	10/23/2009 8:23:00 AM
Pending	GAT	Electronic	10/23/2009 8:23:14 AM
Batch Not Printed	GAT	Electronic	10/23/2009 8:43:05 AM
Batch Printed	GAT	Electronic	10/23/2009 8:43:38 AM
Unfilled	GAT	Electronic	10/23/2009 9:13:41 AM
Pending	TEU	Electronic	10/23/2009 9:13:49 AM

CALL #: https://libproxy.temple.edu:2343/login?url=http://www.lieber ...

LOCATION: **TEU :: Electronic :: Mary Ann Liebert Online**

TYPE: Article CC:CCG

JOURNAL TITLE: Tissue Engineering Part C: Methods

USER JOURNAL TITLE: Tissue engineering. Part C, Methods

TEU CATALOG TITLE: Tissue engineering. Part C, Methods

ARTICLE TITLE: Finite Element Analysis of Fluid Flow Conditions in Cell Culture

ARTICLE AUTHOR: Salvi, Joshua D

VOLUME:

ISSUE:

MONTH: Sep

YEAR: 2009

PAGES: 090924081841022-

ISSN: 1937-3384

OCLC #:

CROSS REFERENCE ID: [TN:161942][ODYSSEY:206.107.42.20/ZCU]

VERIFIED:

BORROWER: **ZCU :: Butler**

PATRON: **Amanda Bielskas**

PATRON ID: asb2154@columbia.edu

PATRON ADDRESS:

PATRON PHONE:

PATRON FAX:

PATRON E-MAIL:

PATRON DEPT:

PATRON STATUS:

PATRON NOTES:

Submission to 'Tissue Engineering'

Finite Element Analyses of Fluid Flow Conditions in Cell Culture

Joshua D. Salvi,[1,2] Jung Yul Lim,[3,4] Henry J. Donahue[5,*]

[1] Department of Bioengineering, Pennsylvania State University, University Park, PA 16802

[2] Weill Cornell Medical College, Cornell University, New York, NY 10021

[3] Department of Engineering Mechanics, University of Nebraska-Lincoln, Lincoln, NE 68588

[4] The Graduate School of Dentistry, Kyung Hee University, Seoul, Korea

[5] Division of Musculoskeletal Sciences, Department of Orthopaedics and Rehabilitation and Center for Biomedical Devices and Functional Tissue Engineering, College of Medicine, Pennsylvania State University, Hershey, PA 17033

(*: corresponding author, Henry J. Donahue)

* Henry J. Donahue: 500 University Drive, Milton S. Hershey Medical Center, Department of Orthopaedics and Rehabilitation, Pennsylvania State University, Hershey, PA 17033

Tel: 717-531-4819; Fax: 717-531-7583; e-mail: hdonahue@psu.edu

ABSTRACT

Numerous studies in tissue engineering and biomechanics utilize fluid flow stimulation, both unidirectional and oscillatory, in order to analyze the effects of shear stresses on cell behavior. However, it has typically been assumed that these shear stresses are uniform and that cell and substrate properties do not adversely affect these assumptions. With the increasing utilization of fluid flow in cell biology, it would be beneficial to determine the validity of various experimental protocols. Since it is difficult to determine the velocity profiles and shear stresses empirically, we utilized the finite element method (FEM). By using FEM, we determined the effects of cell confluence on fluid flow, the effects of cell height on the uniformity of shear stresses, apparent shear stresses exhibited by cells cultured on various substrates, and the effects of oscillatory fluid flow relative to unidirectional flow. FEM analyses could successfully analyze flow patterns over cells for various cell confluence and shape and substrate characteristics. Our data suggest the benefits of the utilization of oscillatory fluid flow and the use of substrates that stimulate cell spreading in the distribution of more uniform shear stresses across the surface of cells. Also, we demonstrated that cells cultured on nanotopographies are exposed to greater apparent shear stresses than cells on flat controls when using the same fluid flow conditions. FEM thus provides an excellent tool for development of experimental protocols and the design of bioreactor systems.

INTRODUCTION

One of the key strategies in tissue engineering is mimicking the in vivo environment in vitro to optimize cell growth and tissue formation. Typically, cells are cultured in vitro on flat surfaces, such as tissue culture polystyrene, glass slides, etc. Not surprisingly, cells cultured on these substrates behave differently than cells in vivo. A number of substrates that mimic the in vivo environment have been produced. One method is an alteration of surface topography at either a micro- or nanoscale using self-organizing or lithographic techniques. Topographical changes become a key in controlling cell morphology, cytoskeletal organization, and protein adsorption at the cell-surface interface. In addition to topographical engineering of substrates, biofunctionalization allows a firm cell anchorage through peptide motifs that bind to integrins or other cell adhesion molecules. Alternatively, these peptides can be covalently linked to the surface, or peptide linkers can be used to bind these proteins to the material surface. Typically, a combination of these biomimetic properties would be incorporated into the ideal substrate. However, each property and technique must be analyzed independently (4,15,16).

Previous studies in our laboratory have demonstrated that polymer demixed nanotopographies induce differential cell responses as a function of nanotopographic scale. For example, human fetal osteoblastic cell (hFOB) adhesion and proliferation are significantly greater on 10-30 nm high nanoislands than on flat control films (20,21). This demonstrates that osteoblastic cells preferentially adhere to and grow on specific nanotopographies. Also, we found that surface nanoscale topography influences integrin and focal adhesion protein synthesis by osteoblastic cells (23). These data demonstrate that substrate nanotopography is an important mediator of initial cell adhesion, proliferation and potentially differentiation.

In addition to nanotopography we have demonstrated that fluid-flow-induced shear stress can increase bone cell, including mesenchymal stem cell, proliferation (29, 30). Furthermore, we have shown that osteoblastic MC3T3-E1 cells cultured on 11-38 nm high nanoislands displayed significantly greater elastic moduli relative to those cultured on flat polystyrene or plasma-cleaned glass surfaces (32). This change in elastic modules would be expected to alter the sensitivity of cells to biophysical signals. This led us to develop the hypothesis that a combination of biophysical signals and surface nanotopography would result in increased apparent shear stress effects possibly due to the increased elastic moduli of cells cultured on nanotopographies. However, it is possible that culture of cells on nanotopographies alters the shear stress to which the cells are exposed rather than affecting the cell's sensitivity to shear stress. To address this we analyzed fluid flow profiles and induced shear stresses for cells cultured under various conditions including on nanotopographies.

Fluid flow profiles and induced shear stresses can be analyzed with the help of the finite element method (FEM, or finite element analysis) (1-9). FEM allows for the discretization of complex geometries, allowing for greater flexibility, in the study of mechanics, than finite volume methods. Typically, finite element analyses require the use of computer technology for discrete approximations (10).

FEM requires the use of computational methods, and in this particular study COMSOL Multiphysics (formerly FEMLAB) has been utilized. COMSOL is unique in that it can not only analyze complex geometries by finite element analysis but it can also couple multiple physical modules into a single geometry. The program was initially developed by Germund Dahlquist at the Royal Institute of Technology in Stockholm, Sweden (12). This technique grants the ability

to couple structure stress-strain analyses with the fluid mechanics of a geometry as implemented by steady-state Navier-Stokes equations (13).

Finite element analyses are integral to the estimation of physical properties in complex geometries. In tissue engineering, these analyses are commonly used for the simulation of bioreactor systems, e.g., spinning flask bioreactors and perfusion flow bioreactors. However, fluid flow over cells cultured on nanoscale topographies has yet to be analyzed through finite element methods. Regarding the simulation of flow perfusion bioreactors, the most common method used for fluid flow stimulations is the Lattice-Boltzmann method, where physical three-dimensional space is broken into a number of nodes. The important factor to consider, however, is that fluid flow simulations with the Lattice-Boltzmann method simplifies the Navier-Stokes equations to a second-order set of equations and assumes that all fluids are Newtonian fluids. As a result, the calculations with these methods are very rough estimates (14). The methods used in the literature were successful in the simulations of velocity fields through bioreactors, and in these simulations shear stresses were coupled with velocities at the solid-fluid interface. In coupling empirical data regarding scaffold properties and then analyzing flow fields, the flow field properties existing within the flow perfusion bioreactors could thus be estimated. However, most of the bioreactor studies omitted these simulation steps prior to bioreactor design.

In this study we completed FEM simulations of fluid flow profiles and induced shear stress on cells under various cell and substrata conditions including cell confluence, cell height, and substrate nanotopography. The objective was to compare these various cell properties under both unidirectional and oscillatory fluid flow conditions to bring to light any differences in biophysical signals imposed on cells. It was hypothesized that unidirectional flow will have patterns leading to non-uniform stresses along surfaces not seen under oscillatory conditions.

Additionally, fluid flow should impose more uniform stresses along the surfaces of cells with lower height. Finally, experimental data describing the elastic moduli of cells cultured on various substrates allows us to predict that these stiffer cells will have greater responses to biophysical signals. This is to say that fluid flow will impose greater shear stresses on those cells with greater elastic moduli. Such hypotheses have not been confirmed in the laboratory, and FEM provides the best method to elucidate such questions.

FEM simulations are introduced as a novel method in tissue engineering not typically used. By coupling experimental data with data created *in silico*, insights not typically witnessed in the laboratory can be brought to light. Phenomena in fluid flow patterns and biophysical signals witnessed in our laboratory have been elucidated in this manuscript. This method will greatly help to optimize bioreactor design that utilizes fluid flow and nanotopographies in musculoskeletal tissue engineering.

MATERIALS AND METHODS

COMSOL Multiphysics (COMSOL, Inc., Burlington, MA, USA) was utilized to simulate the two-dimensional microenvironment of cells cultured on nanoscale topographies. Included in the comparison were varying levels of cell confluence from flat to 100% confluent, flow patterns over cells that differ in cell height from 1.5 microns to 7.5 microns based upon the geometry of human mesenchymal stem cells, effects of differing elastic moduli of cells cultured on various substrata, and analyses of general flow patterns over generalized bumps in fluid flow. The dimension of the flow chamber used in these simulations was set at L = 3 mm and the height = 0.7 mm.

When comparing the cells cultured on multiple substrata, elastic modulus data from Hansen et al. (32) were utilized as inputs for the moduli of cells on these surfaces. This approach allowed for an indirect study of cell stress on multiple substrata without explicitly modeling the various surfaces. Such an approach allows for a coupling of *in vitro* and *in silico* data from finite element analyses. Hansen's study compared cell stiffness of human fetal osteoblastic (hFOB) cells cultured on various substrata. It was assumed in this simulation that cells cultured on flat polystyrene had an average modulus of 4000 Pa, those on plasma-cleaned glass had a average modulus of 7000 Pa, cells on 11 nm nanoislands had an elastic modulus of 9000 Pa, and those cultured on 38 nm nanoislands had a modulus of 12000 Pa. In using these data, the effects of fluid flow over cells cultured on various substrata using the moduli as the independent variable could be compared. This becomes interesting when considering two flat surfaces such as flat polystyrene and plasma-cleaned glass that exhibit the same topographies but very different cell stiffness responses. Furthermore, shear stresses along the surfaces of cells cultured on various nanoscale topographies were compared by modeling the cell stiffness as opposed to the surface morphology. In doing so, the required computing power and time to solution were greatly reduced. Incompressible Navier-Stokes fluid flow was coupled with a stress-strain analysis to determine the apparent shear stresses induced on the surfaces of these cells.

When analyzing oscillatory fluid flow, one must ensure that the flow remains laminar if assumptions and equations are to hold. The maximum Reynolds number was 16.302 using the following criteria:

$$\text{Inlet Pressure: } P_{inlet} = 0.5k \times \cos(\omega t) + P_{atm} \quad (1)$$

$$\text{Outlet Pressure: } P_{outlet} = -0.5k \times \cos(\omega t) + P_{atm} \quad (2)$$

$$\text{Constants: } \omega = 2\pi\ rad/s;\ P_{atm} = 131\ kPa;\ k = 4000\ N/m^3 \quad (3)$$

The inlet and outlet pressures were increased by a positive atmospheric pressure (P_{atm}) at 131 kPa, since it is assumed that atmospheric pressure acted at both ends of the bioreactor. However, these pressures were opposite one another in the sinusoidal term. The angular frequency of oscillation (ω) was 2π rad/s, correlating to a period of oscillation of one second. Additionally, this term was scaled by a constant (k) of 4000 N/m^3. This number was chosen in order to minimize the maximum Reynolds number and to simulate flow rates similar to those in the laboratory.

The pressure difference in unidirectional flow was a constant at $\Delta P = \rho g L$, where ΔP is the pressure difference across the bioreactor, ρ is the density of the fluid in kg/m^3 (in this case, water was utilized with ρ = 1000 kg/m^3), g is the acceleration due to gravity (g = 9.81 m/s^2), and L is the length of the bioreactor being simulated in meters.

The incompressible Navier-Stokes equations and the assumptions include:

$$\rho(\partial u/\partial t)+\rho \boldsymbol{u}\nabla \boldsymbol{u} = \nabla[-\rho \boldsymbol{I} + \mu(\nabla \boldsymbol{u} + (\nabla \boldsymbol{u})^{T})] + \boldsymbol{F} \qquad (4)$$

$$\nabla \boldsymbol{u} = \boldsymbol{0} \qquad (5)$$

$$\mu[\nabla \boldsymbol{u} + (\nabla \boldsymbol{u})^{T}] = \boldsymbol{0} \qquad (6)$$

In the first Navier-Stokes equation, terms can be broken down by those affected by density (ρ), velocity (scalar u or vector $\mathbf{u}$), and viscosity (μ). The first term ($\rho(\partial u/\partial t)$) is the unsteady acceleration term, and the second term ($\rho \boldsymbol{u} \nabla \boldsymbol{u}$) is the convective acceleration term. Together, these terms encompass the inertial component of fluid flow. The terms following the del (∇) operator correspond to the pressure gradient and viscous divergence of stress, respectively. Finally, the variable $\boldsymbol{F}$ accounts for all other body forces in the fluid flow. It can then be assumed that under incompressible conditions, the divergence of velocity (∇u) is zero. With this being true, the viscosity term ($\mu[\nabla \boldsymbol{u} + (\nabla \boldsymbol{u})^{T}]$) is also zero. This greatly simplifies the Navier-Stokes equation to only unsteady acceleration, pressure gradient, and body force terms.

These equations for fluid flow analyses can then be coupled with a stress-strain analysis to determine shear stresses throughout the two-dimensional microenvironment. In the analysis of shear stresses, the normalized von Mises stress was used.

$$\sigma_{VM} = \frac{1}{\sqrt{2}}\sqrt{(\sigma_x - \sigma_y)^2 - (\sigma_y - \sigma_z)^2 - (\sigma_z - \sigma_x)^2 - 6\tau_{xy}^2 - 6\tau_{zx}^2 - 6\tau_{yz}^2} \qquad (7)$$

The von Mises stresses find the differences in normal stresses (σ) in all directions in Cartesian coordinates. The subscripts x, y, and z refer to the particular face of a three-dimensional surface upon which the normal force acts. Furthermore, the shear stresses (τ) in all directions are included in this equation. The subscripts xy, zx, and yz refer to the direction (second subscript) along a particular face of a three-dimensional surface (first subscript). For example, "xy" refers to a shear stress acting on the x-face in the y-direction. By adding the squares of these terms, the square root of this sum is a normalized stress known as the von Mises stress.

These von Mises stresses were then measured in COMSOL at the surface of the cell. Such stresses act as biophysical signals leading to intracellular responses. For that reason, the stresses resulting from the pressure in fluid flow act as an excellent indicator for cellular response to fluid flow.

All of these data were then analyzed to determine flow patterns, values of shear stresses at multiple locations, and the absolute flow rates in various geometries. Such simulations have been summarized in Table 1, and the corresponding COMSOL model reports have been included in the Supplemental Information (S.A, S.B, and S.C).

RESULTS

Finite Element Analysis of Fluid Flow: Cell Confluence Effects

Our simulation in COMSOL Multiphysics analyzed the effects of cell confluence on fluid flow patterns using the unidirectional flow of media. Figure 1 depicts the macroscopic view of flow over cells with varying levels of confluence. We note that cells are cultured on the

substrate and the substrate is placed inside a flow chamber. The flow pattern inside the chamber is displayed with colors and arrows, and the cells are shown as white semi-circles at the bottom of the flow pattern. Note that there were very little differences in flow patterns within the bioreactor, mostly with 50% and 100% confluence at the upper boundary of the bioreactor. However, these differences in flow patterns were not detected in a macroscopic view. Thus, a microscopic view of flow over cells was analyzed.

Figure 2 depicts the microscopic view of flow over cells partially confluent to varying degrees and 100% confluent. Note the velocity field contour lines in addition to the colored surfaces. Figures 2A and 2B depict unidirectional fluid flow of cells that are 50% confluent and 100% confluent, respectively. In both cases, a cell was located at the entrance to the flow region. In doing so, this initial bump in the flow significantly altered the flow patterns such that flow was at or near zero along the surfaces of following cells. Thus, it could be argued that the shear stresses along the surfaces of these cells would be significantly lower.

Figure 2C depicts the flow along the cells when a cell height is relatively high (10 μm) and cells are highly confluent. Note that the flow is nonzero along the upper region of the cells, but the space between cells exhibited flow rates at or near zero. Thus, this unidirectional flow simulation suggests that the shear stresses between cells in this condition (high cell height and high confluence) are also at or near zero. Therefore, the shear stresses along the arc-length of such cells are non-uniform.

Figure 2D displays the flow pattern beyond the entrance region when the cell height is low (2.5 μm) and 50% confluent. In this case, the lack of flow along the cell surface observed in Figures 2A and 2B becomes minimal. Furthermore, some flow occurs over a greater surface area of the cells, and the shear stresses become more uniform along the cell arc-length when

compared with those in Figure 2C. Therefore, these data suggest that cells with a lower confluence and with a well spread cell morphology will undergo more uniform shear stresses under fluid flow than cells that are more confluent and have a less well-spread morphology.

Finite Element Analysis of Fluid Flow: Cell Height Effects

As we briefly introduced in the previous section, cell height also affects the flow pattern inside the fluid flow chamber. It has been reported that various biomaterials characteristics affect cell spreading behavior and thus alter cell shape parameters including cell height, area, Feret's diameter, etc. Material surface chemistry and surface energy dependent hydrophobicity may be one important mediator of the cell spreading (14).

First, we consider the extreme case that cell spreading is very low and cell height is very high (20 μm) and such a cell is exposed to unidirectional flow (Figure 3). This reveals a few important characteristics. First, a very high cell height leads to a lack of flow at the edge of the cell on both sides of flow, shown as blue portions in Figure 3. This leads to a concentration of higher shear stresses at the upper surface of the cell. This would predict that the shear stresses cells experience would be non-uniform in nature. Oscillatory fluid flow would thus be relatively more beneficial than unidirectional flow in distributing the shear stresses along the surface of these cells.

Furthermore, eddies begin to form in the distal region of flow, just beyond the right side of the cell in the flow field. This will lead to turbulence if velocity is increased, and such turbulence could hypothetically fabricate negative effects on cell adhesion, distribution of shear stresses, and conservation of energy. In other words, the assumptions necessary for reproducibility in experimental protocols would break down if such turbulence were to occur. As

a result, this extreme condition predicts that oscillatory fluid flow provides a more consistent and beneficial experimental condition than protocols utilizing unidirectional constant or unidirectional peristaltic fluid flow of media over cells with larger height.

Therefore we then simulated oscillatory fluid flow over cells with varying heights. The purpose was to determine the general differences between relative shear stresses induced by oscillating fluid flow on cells with varying potential to spread. We hypothesized that cells with larger cell height would be exposed to greater shear stresses but concentrated near the center of the cell. This hypothesis stemmed from the preliminary simulation shown in Figure 3. As shown in Figure 4, when oscillatory fluid flow was utilized, the flow profiles were all disturbed showing little difference among the various conditions except at the cell surfaces. However, as the cell height was increased, the fluid flow profile was further disturbed.

We then quantified the von Mises stresses from these oscillatory fluid flow simulations at various portions of the cells (Figure 5). When oscillatory fluid flow (1 Hz) was applied, stresses with sinusoidal patterns were observed from t = 0.0 s to t = 3.0 s for all cell portions (center, left, right) and for all cell heights. If we measure stresses at the center of the cell (Figure 5, top), the amplitude of this sinusoidal pattern varies more for cells with the larger cell heights, having the greatest peak amplitude at ca. 120 dyn/cm^2. On averaging these data (top bar graph) it was observed that greater shear stresses would be concentrated at the cell center when the cell height is the highest. In the case that the cell height is 'high', the average stress value was not that high but the amplitude and maximum stress values were relatively greater than the cases of cell height is 'lowest' and 'low'.

Figure 5, middle, depicts the same data but at the left portion of the cell under oscillating fluid flow for 3.0 seconds. Unlike the cell center, the von Mises stresses at the leftmost point on

each cell from t = 0.0 s to t = 3.0 s was very similar in its sinusoidal pattern among cells with varying height. In fact, it becomes very difficult to analyze these time-dependent data at this location. Nevertheless, one can easily locate very high shear stresses for cells with smaller heights. These can be clearly seen in the averaged stress data. One can observe that for cells with larger heights lower shear stresses exist at the leftmost point of adhesion. Considering oscillatory fluid flow was utilized, similar trends in data were displayed at the distal location in the flow field (Figure 5, bottom). This further indicates the benefit of oscillatory fluid flow over unidirectional flow where such consistency at both cell sides would not be exhibited as in Figure 3. Therefore, these data suggest the benefits of utilizing of oscillatory fluid flow and the use of substrates that stimulate cell spreading in the distribution of more uniform shear stresses across the surface of cells.

Finite Element Analysis of Fluid Flow: Cells on Nanotopographies

FEM with COMSOL Multiphysics was employed to analyze oscillatory fluid flow over cells cultured on nanotopographies (polystyrene/polybromostyrene, PS/PBrS 40/60 w/w demixed films) and flat controls (plasma-cleaned glass, flat polystyrene). The nanotopographies used for simulation in this study were 11 nm and 38 nm high nanoislands. Though the nanoscale substrata were not explicitly simulated, a more indirect approach was taken for prediction of apparent shear stress. According to past experimental data (15), it was assumed that cells cultured on these surfaces have the approximate elastic moduli values as noted in the Materials and Methods section. The purpose of these simulations was to analyze the differences in apparent shear stresses under the same flow conditions. In order to do so, all cells were simulated at the same smaller cell height (2.5 μm) and by using oscillatory fluid flow conditions. As shown previously,

a smaller cell height and oscillatory fluid flow exhibit the greatest level of shear stress distribution (Figures 4, 5).

Although it would be predicted that these assumptions will hold true, it is still helpful to verify these assumptions by initially analyzing the velocity fields and von Mises stress gradients at various time points and on the various substrata. In Figure 6, it appears there are no significant differences in the velocity field as demonstrated by the grayscale streamlines and the red arrows. The middle column, at t = 2.3 seconds, depicts the peak velocity in the sinusoidal fluid flow simulation. This time point was chosen due to the fact that oscillatory pressure becomes maximum at t = 2.3 seconds. Specifically, the cosine function is nearest 1 at this time with a frequency of 2π rad/sec. Again, even at the peak flow, there is no significant difference in velocity field and von Mises stress distribution among the various substrates. This allows for a consistent examination of the apparent shear stresses along the cell surface.

In order to analyze the average shear stresses along the cell surface, the von Mises stress was quantified for each element along the arc length of the cell surface with the cellular elastic moduli values assumed. Each of these elements was then averaged with the others to find this apparent shear stress at the cell surface. These average shear stresses at t = 0.5, 2.3, and 3.0 s are shown in Figure 7. These correspond to velocities of 2.07 cm/s. 8.81 cm/s, and 2.52 cm/s, respectively. Peak pressure gradients of corresponded with greater velocity fields.

At t = 0.5 s, there were significant differences in apparent shear stresses that the cell will experience on various substrate surfaces. Cells cultured on 38 nm nanoislands displayed significantly greater shear stresses than both the cells cultured on plasma-cleaned glass and on flat polystyrene. Furthermore, cells cultured on 11 nm nanoislands were also significantly greater in apparent shear stresses than those cultured on flat polystyrene. Taken together, at t = 0.5 s the

apparent shear stresses experienced by cells under oscillatory fluid flow were significantly greater when the cells were on nanoscale topographies relative to cell on flat surfaces. At t = 2.3 s, cells cultured on 38 nm nanoislands were once again exposed to significantly greater shear stress than those cultured on plasma-cleaned glass and flat polystyrene, while there was no significance for cells cultured on 11 nm nanoislands. These data suggest that the significant increase in apparent shear stresses is upheld under peak flow conditions. At t = 3.0 s, the significance in data was similar to the t = 0.5 s time point.

It is interesting that cells cultured on 11 and 38 nm nanoisland topographies exhibited significantly greater apparent shear stresses under the same oscillatory flow conditions than their flat counterparts. This increase in apparent shear stress could thus be correlated to other findings of increased mechanosensitivity of cells cultured on these nanoscale substrata when compared with flat controls (24, 26).

If various substrata were utilized, but the elastic modulus was not affected by such substrata, differences in flow profiles would be negligible. As a result, it would be predicted that holding the modulus constant while altering nanoscale topography would not significantly affect the apparent shear stresses experienced by cells.

DISCUSSION

FEM simulations were utilized in this study in order to analyze fluid flow patterns inside a cell cultured flow chamber. Firstly, we examined the variability of fluid flow patterns among various levels of cell confluence. At the macroscopic level, no significant differences were noted. Thus, cell confluence was concluded to have no major effect on the flow profiles in bioreactors.

However, microscopic analyses demonstrated that little to no flow would occur between highly confluent cells. When cell confluence was decreased, fluid flow could more easily occur between cells. Furthermore, cells in the entrance region of flow in the bioreactor would alter the patterns of flow over cells downstream. It would thus be assumed that lower levels of confluence, 50% confluent or less, would be optimal in the design of bioreactors utilizing such fluid flow. This lower confluence allows for a better distribution of fluid flow across cell surfaces and thus a better distribution of wall shear stresses. However, we suspect that the lower confluence may be a trade-off considering potential stimulatory effects from cell-to-cell communication. Thus, there may be an optimal cell confluency level that allows both uniform, positive fluid flow effects and cell-to-cell communication effects.

As regards cell height effects, FEM demonstrated a lack of flow in the distal region of cells when the cell height is greater. Furthermore, these data suggest that oscillating fluid flow used in some bioreactor systems (8, 16, 17) would be more beneficial than constant or peristaltic unidirectional fluid flow found in similar bioreactors due to a more uniform distribution of shear stresses along cell surfaces (9, 18-22). In analyses using oscillating fluid flow conditions, cells with larger heights lead to more concentrated shear stresses near the center of the cell. With decreasing cell height (relevant to increased cell spreading), the shear stresses at the center of the cells decreased on average and the shear stresses at the left and right of the cell increased. These relative changes imply a more efficient distribution of shear stresses with decreasing cell height. Though the method by which cells sense shear stress remains yet to be elucidated, it has been assumed that stresses taken across the surface area of the cell as opposed to a concentration at one location would prove to be more beneficial. Additionally, these data may explain why cells with greater spreading may exhibit a greater response under fluid flow in the laboratory. Taken

together, these data suggest that bioreactors should utilize oscillating fluid flow in combination with substrates that stimulate cell spreading for a better distribution of wall shear stresses in the cell culture system.

Our previous studies demonstrated that cells cultured on various nanoscale topographies will exhibit different biophysical properties, including varying elastic moduli, cell adhesion, and morphology (15, 23, 24). Continuing with finite element analyses utilizing oscillating fluid flow, data from these studies was implemented to determine any potential differences in the apparent shear stresses of cells cultured on these various substrates. The approach taken did not explicitly model the substrates; instead, an indirect approach coupled previous elastic modulus data from *in vitro* studies with the current *in silico* study. This allowed for a comparison of cells on various substrates while limiting the need for computational resources. It was demonstrated in this study that cells cultured on 11 and 38 nm nanoislands exhibited a significantly greater apparent shear stress than cells on flat surfaces. This was due to an increased elastic modulus present in the cells cultured on these surfaces. Since this modulus is the relationship of stress versus strain, an increased modulus will result in decreased strain under the same conditions. In other words, a stiffer cell under the same flow conditions as a less stiff cell will be unable to deform as easily in response to the pressures imposed by flow. For this reason, the apparent shear stress imposed by the flow on the surface of the cell will be greater. Increased cell stiffness is thus correlated with an increased apparent shear stress, and these data support the hypothesis that cells with a greater elastic modulus will exhibit increased apparent shear stresses under oscillating fluid flow conditions.

The success of finite element analyses was witnessed in the examination of factors not easily determined empirically through the demonstration that cells cultured on nanotopographic

substrata exhibited increased apparent shear stresses relative to cells on flat surfaces. Furthermore, FEM was used in such a way that an experiment could be set up to empirically validate these results through parallel analyses. Thus, these methods provide an excellent segue into exploring future routes of study.

A key element of the data presented was the demonstrated benefit of oscillating fluid flow as a superior method to its unidirectional counterpart. Flow is more evenly distributed in the bioreactor system over time, leading to a better distribution of shear stresses across cell membranes. This distribution allows such systems to be more predictive due to a better estimate of the flow rates and shear stresses at the walls of a bioreactor. Thus, it can be concluded that oscillating fluid flow provides greater benefits than constant or peristaltic unidirectional fluid flow systems.

Our data demonstrate that FEM can be successfully utilized to analyze flow patterns over cells culture under various conditions. FEM provides an excellent tool in the prediction of experimental protocols and the design of bioreactor systems. Though the bioreactor system presented here was simulated as a two-dimensional substrate simplified to a single plane, FEM can easily be expanded to analyze more complex geometries. When discussing the difference in perfusion of three-dimensional bioreactor systems, this same method could provide insight not easily acquired through empirical methods.

References:

1. Alvarez-Barreto JF, Linehan SM, Shambaugh RL, Sikavitsas VI. Flow perfusion improves seeding of tissue engineering scaffolds with different architectures. Ann Biomed Eng.35:429-42. 2007.
2. Bancroft GN, Sikavitsas VI, Mikos AG. Design of a flow perfusion bioreactor system for bone tissue-engineering applications. Tissue Eng.9:549-54. 2003.
3. Holtorf HL, Sheffield TL, Ambrose CG, Jansen JA, Mikos AG. Flow perfusion culture of marrow stromal cells seeded on porous biphasic calcium phosphate ceramics. Ann Biomed Eng.33:1238-48. 2005.
4. McMahon LA, O'Brien FJ, Prendergast PJ. Biomechanics and mechanobiology in osteochondral tissues. Regen Med.3:743-59. 2008.
5. Panda P, Ali S, Lo E, Chung BG, Hatton TA, Khademhosseini A, et al. Stop-flow lithography to generate cell-laden microgel particles. Lab Chip.8:1056-61. 2008.
6. Riddle RC, Donahue HJ. From streaming-potentials to shear stress: 25 years of bone cell mechanotransduction. J Orthop Res. 2008.
7. Riddle RC, Hippe KR, Donahue HJ. Chemotransport contributes to the effect of oscillatory fluid flow on human bone marrow stromal cell proliferation. J Orthop Res.26:918-24. 2008.
8. Riddle RC, Taylor AF, Donahue HJ. Fluid flow assays. Methods Mol Biol.455:335-45. 2008.
9. Zhao F, Ma T. Perfusion bioreactor system for human mesenchymal stem cell tissue engineering: dynamic cell seeding and construct development. Biotechnol Bioeng.91:482-93. 2005.
10. Tang H. Mathematics of the Finite Element Method. 1995.
11. Strang G. An Analysis of the Finite Element Method: Prentice Hall, Inc.; 1973.
12. Mathematics SflaA. Obituary: Germund Dahlquist. 2005.
13. AB. C. COMSOL Multiphysics. 2008.
14. Porter B, Zauel R, Stockman H, Guldberg R, Fyhrie D. 3-D computational modeling of media flow through scaffolds in a perfusion bioreactor. J Biomech.38:543-9. 2005.
15. Hansen JC, Lim JY, Xu LC, Siedlecki CA, Mauger DT, Donahue HJ. Effect of surface nanoscale topography on elastic modulus of individual osteoblastic cells as determined by atomic force microscopy. J Biomech.40:2865-71. 2007.
16. Donahue TL, Haut TR, Yellowley CE, Donahue HJ, Jacobs CR. Mechanosensitivity of bone cells to oscillating fluid flow induced shear stress may be modulated by chemotransport. J Biomech.36:1363-71. 2003.
17. Alford AI, Jacobs CR, Donahue HJ. Oscillating fluid flow regulates gap junction communication in osteocytic MLO-Y4 cells by an ERK1/2 MAP kinase-dependent mechanism small star, filled. Bone.33:64-70. 2003.
18. Chromiak JA, Shansky J, Perrone C, Vandenburgh HH. Bioreactor perfusion system for the long-term maintenance of tissue-engineered skeletal muscle organoids. In Vitro Cell Dev Biol Anim.34:694-703. 1998.
19. Li X, Li D, Wang L, Wang Z, Lu B. [Development of rotating perfusion bioreactor system and application for bone tissue engineering]. Sheng Wu Yi Xue Gong Cheng Xue Za Zhi.24:66-70. 2007.

20. Ouyang A, Yang ST. A two-stage perfusion fibrous bed bioreactor system for mass production of embryonic stem cells. Expert Opin Biol Ther.8:895-909. 2008.
21. Sikavitsas VI, Bancroft GN, Lemoine JJ, Liebschner MA, Dauner M, Mikos AG. Flow perfusion enhances the calcified matrix deposition of marrow stromal cells in biodegradable nonwoven fiber mesh scaffolds. Ann Biomed Eng.33:63-70. 2005.
22. Wang L, Hu YY, Wang Z, Li X, Li DC, Lu BH, et al. Flow perfusion culture of human fetal bone cells in large beta-tricalcium phosphate scaffold with controlled architecture. J Biomed Mater Res A. 2008.
23. Lim JY, Hansen JC, Siedlecki CA, Hengstebeck RW, Cheng J, Winograd N, et al. Osteoblast adhesion on poly(L-lactic acid)/polystyrene demixed thin film blends: effect of nanotopography, surface chemistry, and wettability. Biomacromolecules.6:3319-27. 2005.
24. Lim JY, Hansen JC, Siedlecki CA, Runt J, Donahue HJ. Human foetal osteoblastic cell response to polymer-demixed nanotopographic interfaces. J R Soc Interface.2:97-108. 2005.

Cell Type	Flow Type	Substrate	Figures	Supplement
Semi-Circular "Bump"	Unidirectional	Flat Polystyrene	1, 2, 3	S.B
1.5 μm High hFOB 3 μm High hFOB 5 μm High hFOB 7 μm High hFOB	Oscillatory	Flat Polystyrene	4, 5	S.A
3 μm High hFOB	Oscillatory	*Plasma-Cleaned Glass *Flat Polystyrene *11 nm Nanoislands *38 nm Nanoislands	6, 7	S.C

Table 1. The varying types of simulations have been summarized here. Preliminary studies used a semi-circular "bump" in unidirectional flow to analyze the effects of confluence on flow patterns. Additionally, these preliminary data were used to examine flow distal to the cell under unidirectional conditions. Varying cell heights of human fetal osteoblastic cells (hFOB) were compared under oscillatory fluid flow conditions to examine the effects of cell height on the relative von Mises stresses imposed upon cells by such flow. Finally, 3 μm high hFOBs were examined under the same oscillatory flow conditions and compared on various substrata. The purpose was to compare the relative von Mises stresses imposed by these flow conditions on cells with varying elastic moduli. All of these analyses and model reports can be found in the figures and supplements noted in the table.

*These substrata were simulated by varying the relative Young's moduli of cells cultured on the various surfaces. Such values were taken from previous experimental data by Hansen et al. (32).

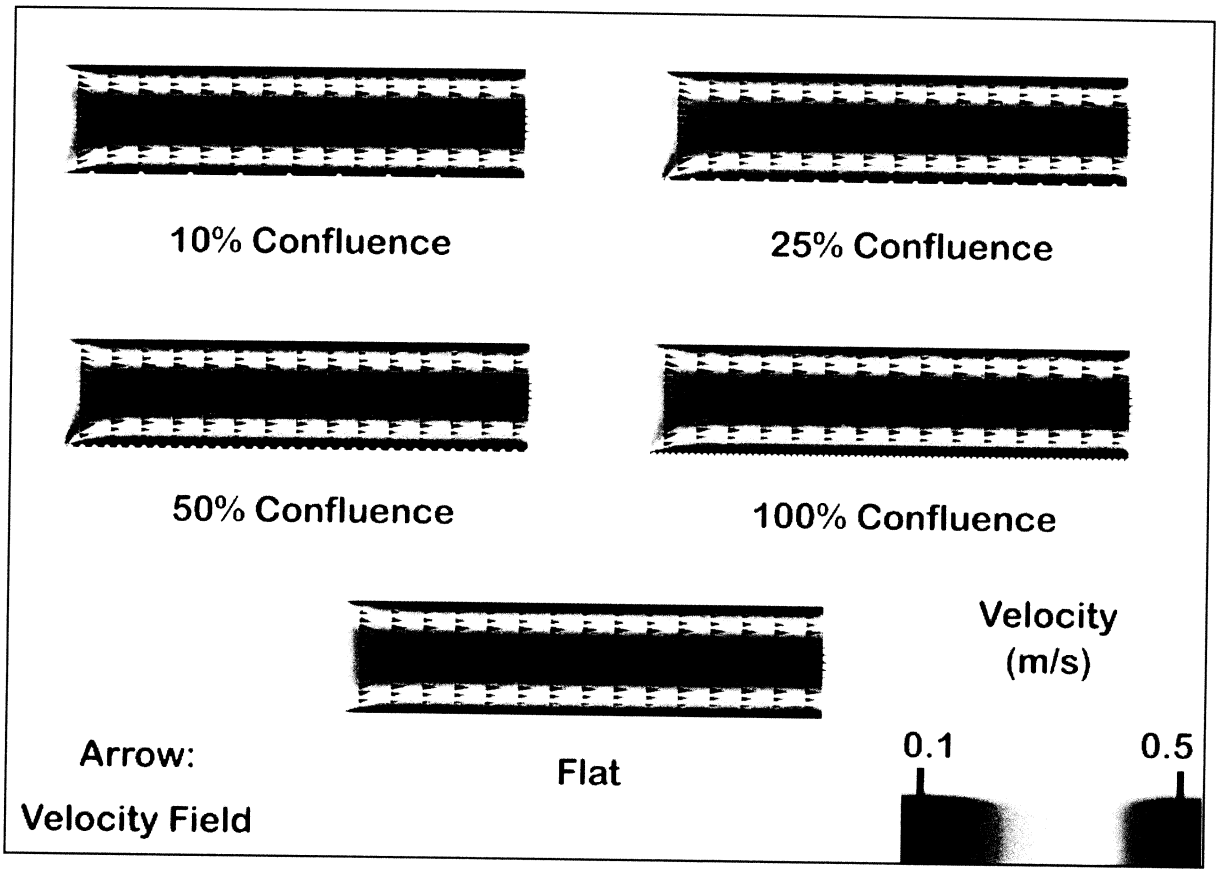

Figure 1. FEM Analysis of cell confluence: macroscopic view. Incompressible Navier-Stokes with a Newtonian fluid was assumed.

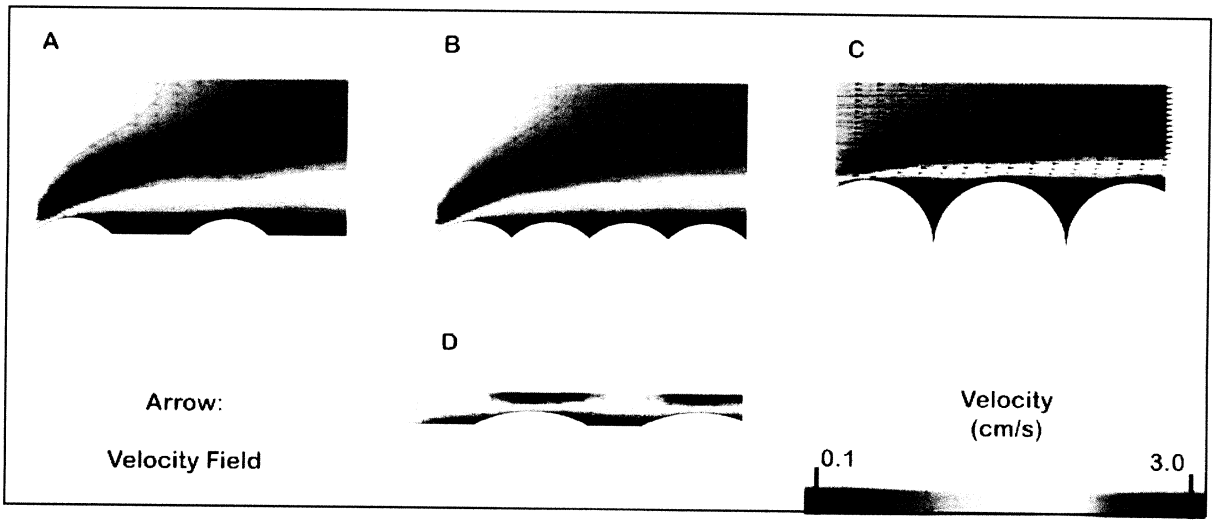

Figure 2. FEM of cell confluence: microscopic view. (A) 50% confluence with cell at entrance to flow field, (B) 100% confluence with cell at entrance to flow field, (C) 100% confluence with a larger cell height, and (D) 50% confluence without cell at entrance.

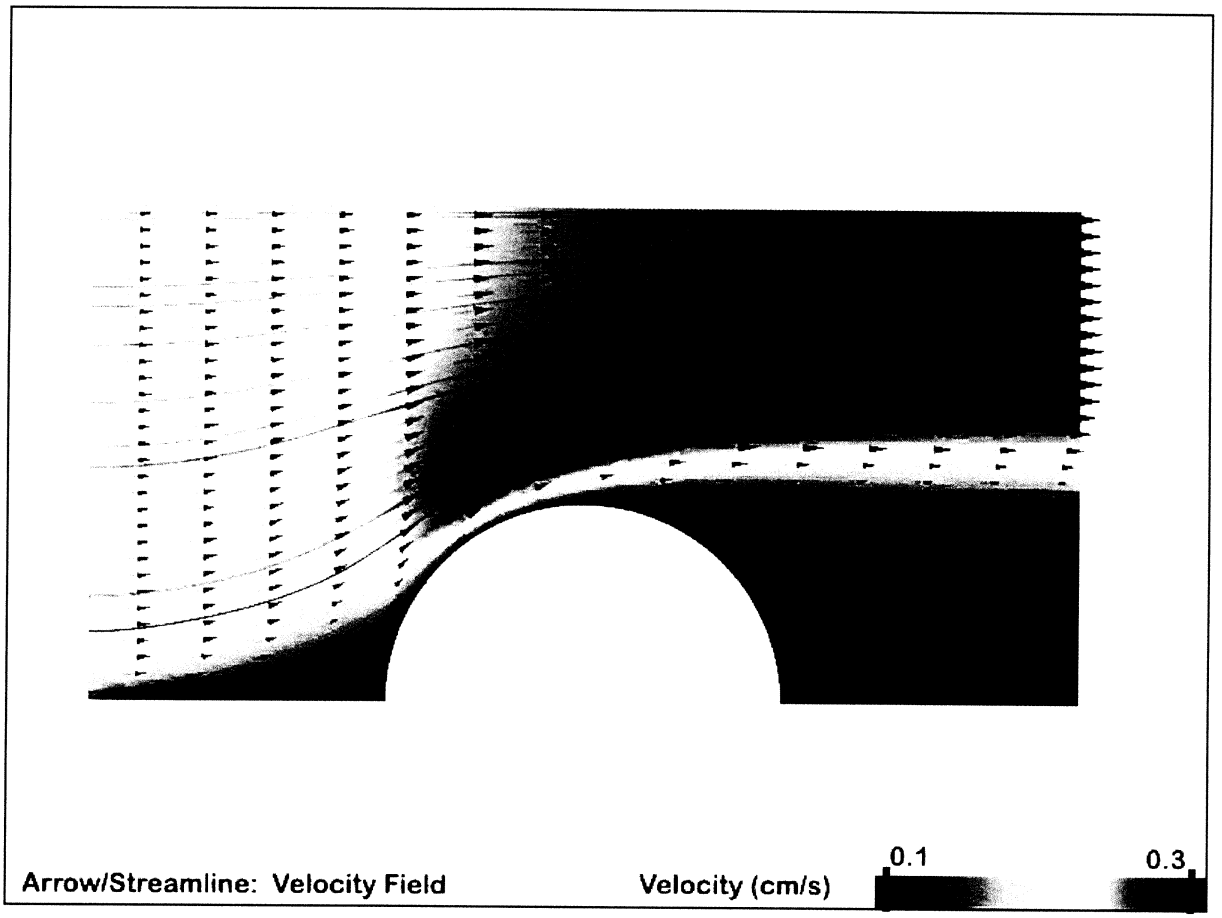

Figure 3. Unidirectional fluid flow pattern over a cell with a large cell height.

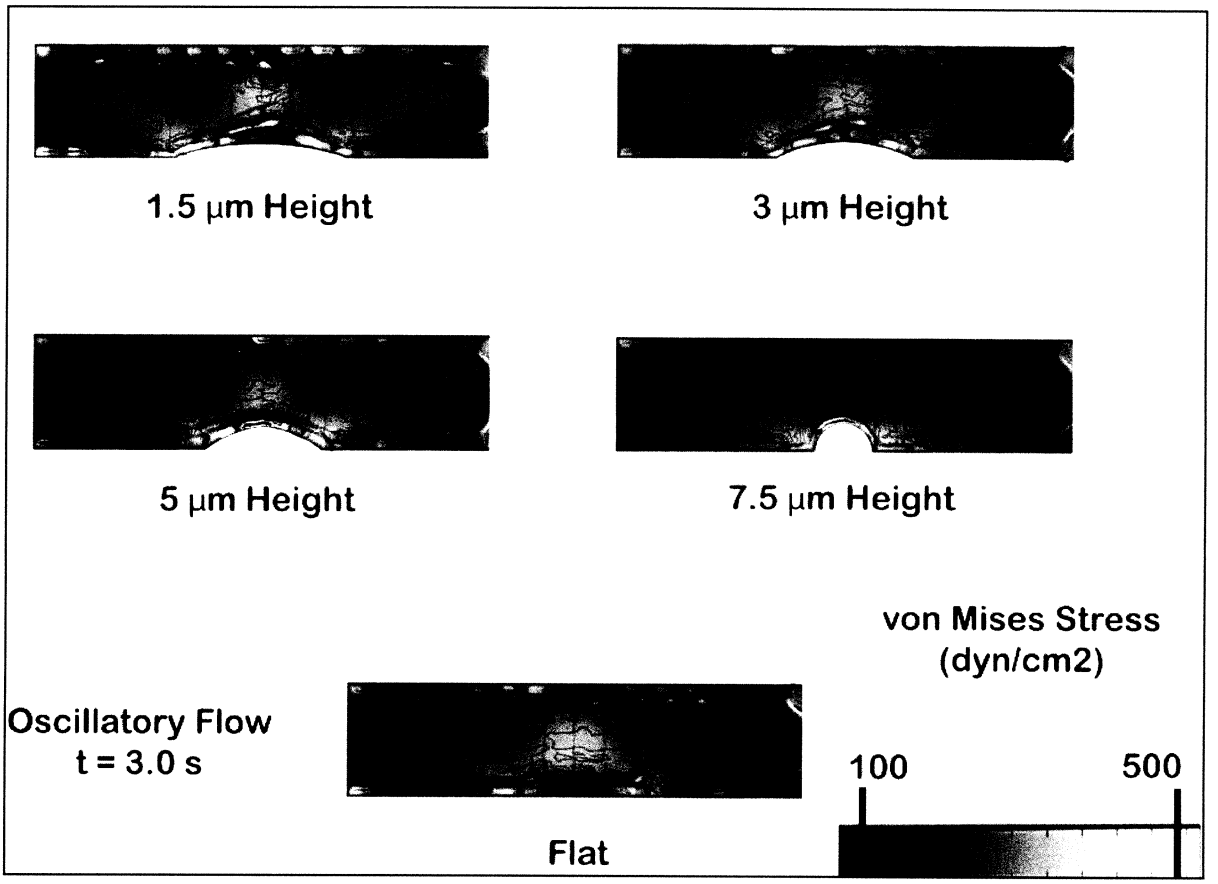

Figure 4. Shear stresses along the surfaces of cells with varying cell height. Oscillatory fluid flow of media was utilized and these data depict the simulation at t = 3.0 seconds. Red arrows depict the velocity field and the grayscale gradient depicts the von Mises stress distribution in the various simulations.

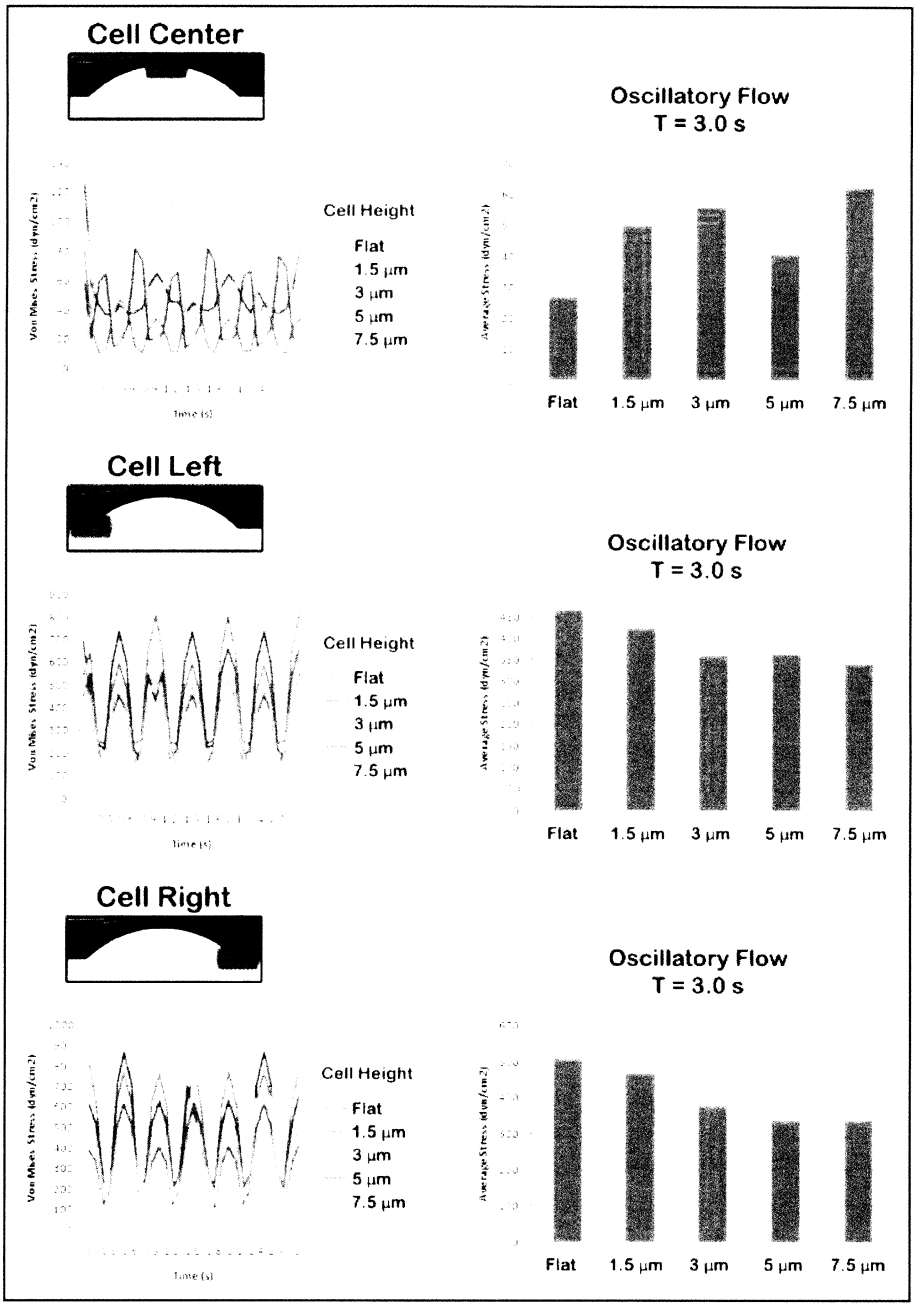

Figure 5. Shear stresses assessed at the cell center (top), cell left (middle), and cell right (bottom) portion over 3.0 seconds, along with the corresponding averages for each variance.

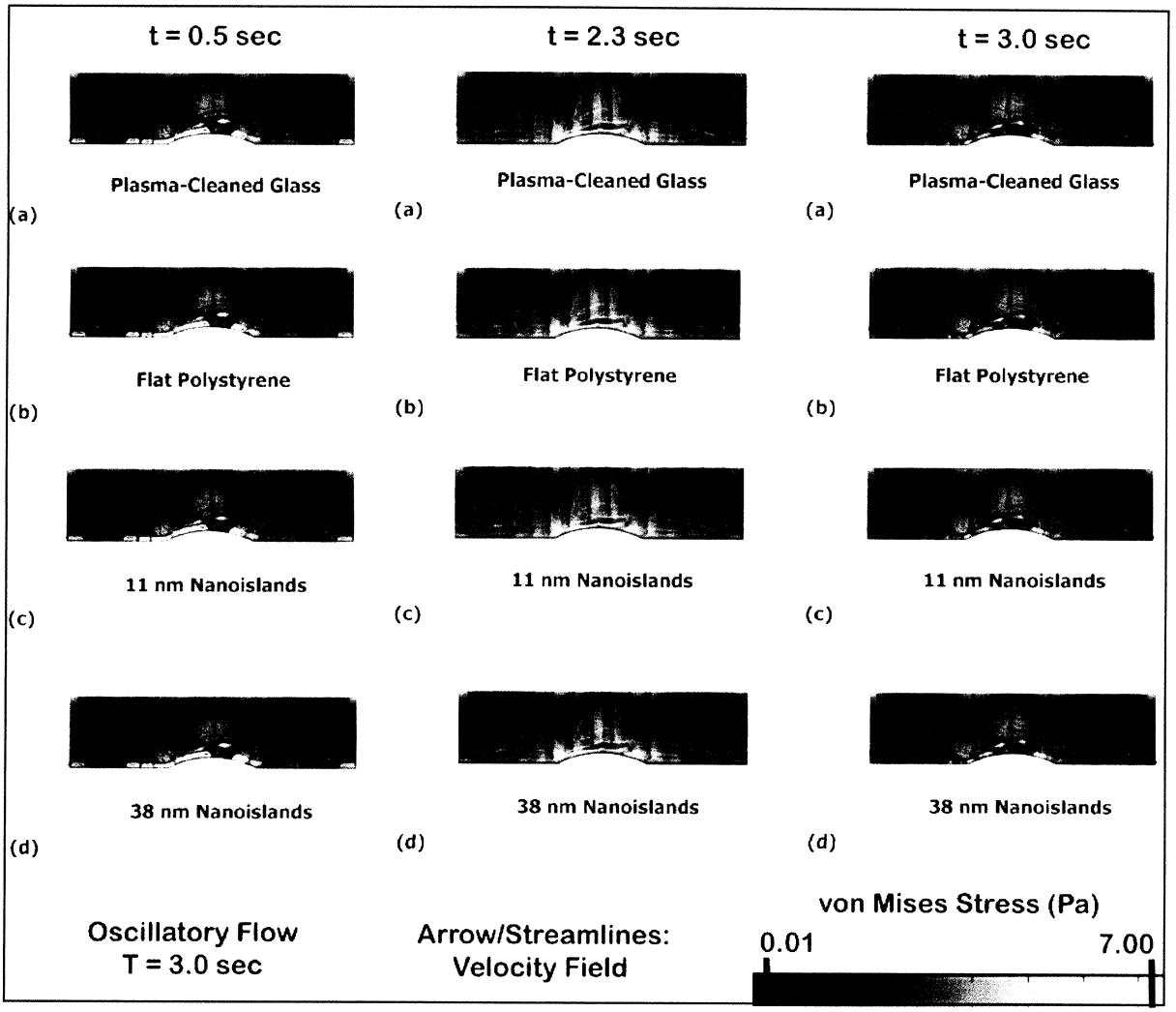

Figure 6. FEM simulation of oscillatory fluid flow on various substrata at t = 0.5 s, t = 2.3 s, and t =3.0 s. Red arrows depict the velocity field, and the grayscale gradient depicts the von Mises stress distribution in the various simulations.

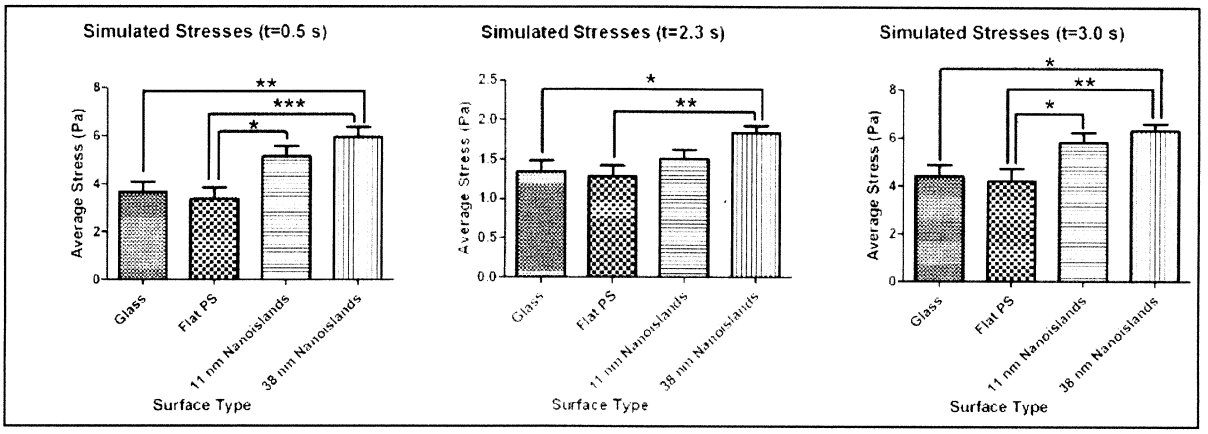

Figure 7. Average shear stresses in the FEM of oscillatory fluid flow over various substrata at t =0.5 s, t = 2.3 s, and t = 3.0 s. (*: $p < 0.05$, **: $p < 0.01$, ***: $p < 0.001$)

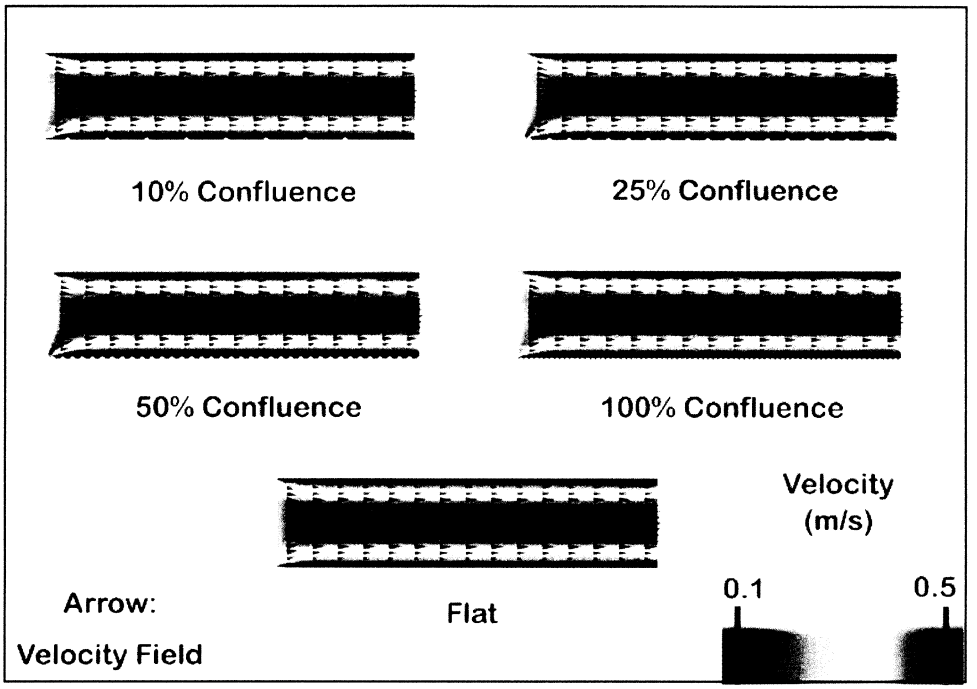

422x298mm (96 x 96 DPI)

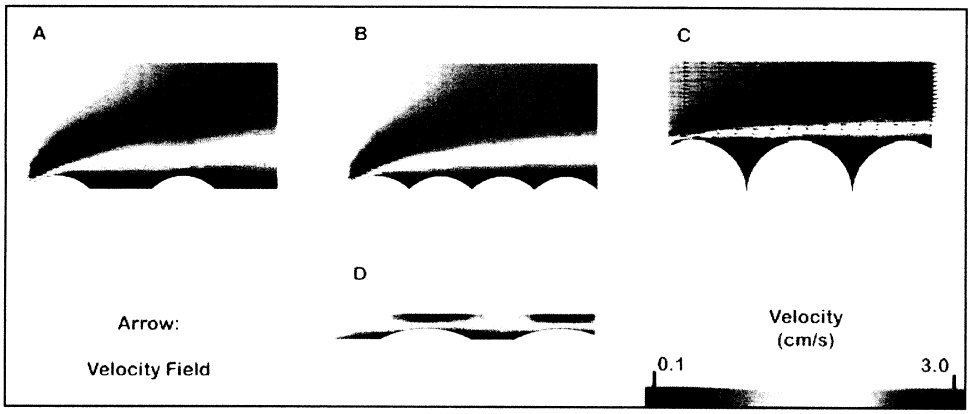

635x264mm (96 x 96 DPI)

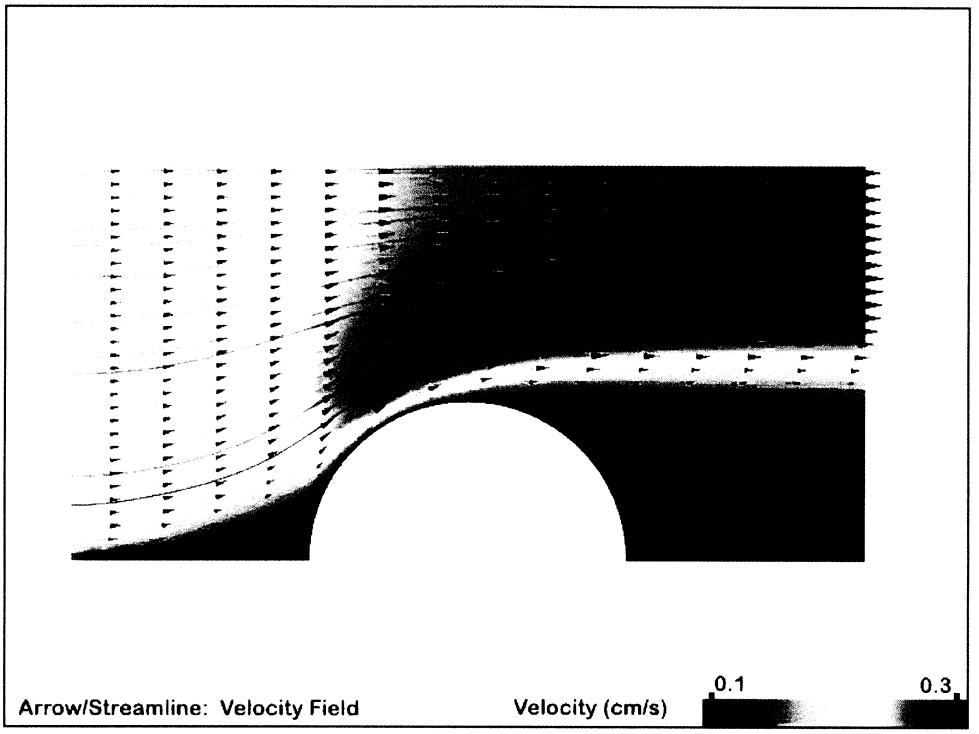

211x158mm (96 x 96 DPI)

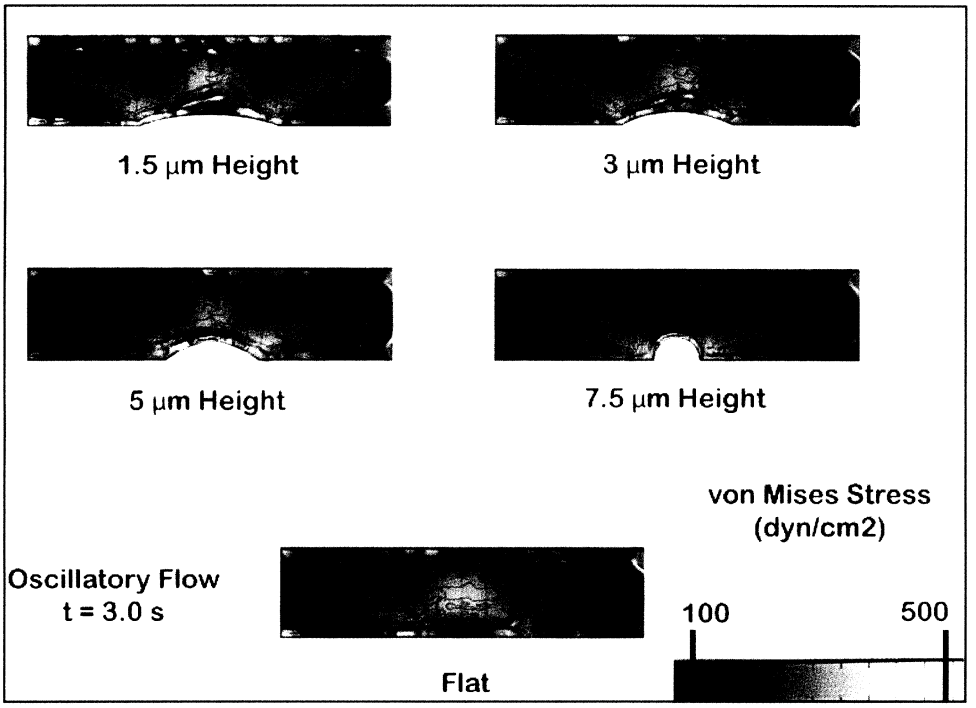

444x322mm (96 x 96 DPI)

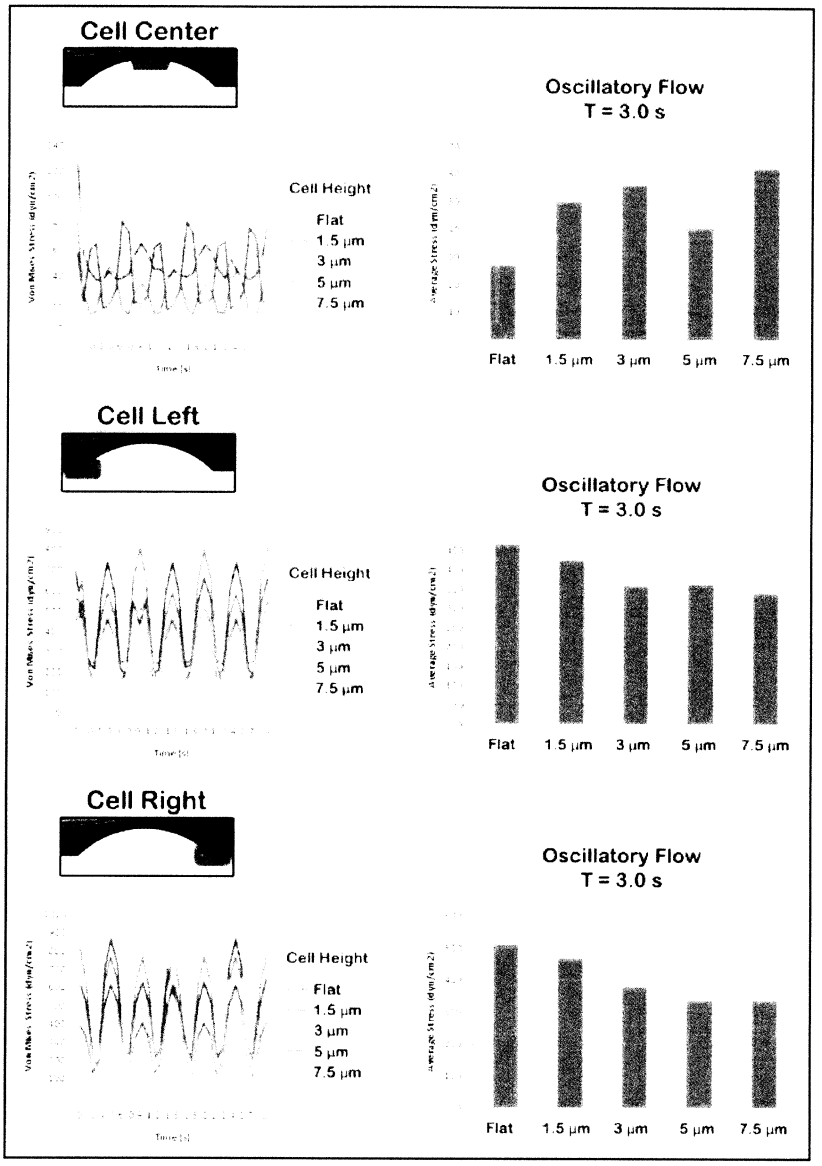

249x357mm (96 x 96 DPI)

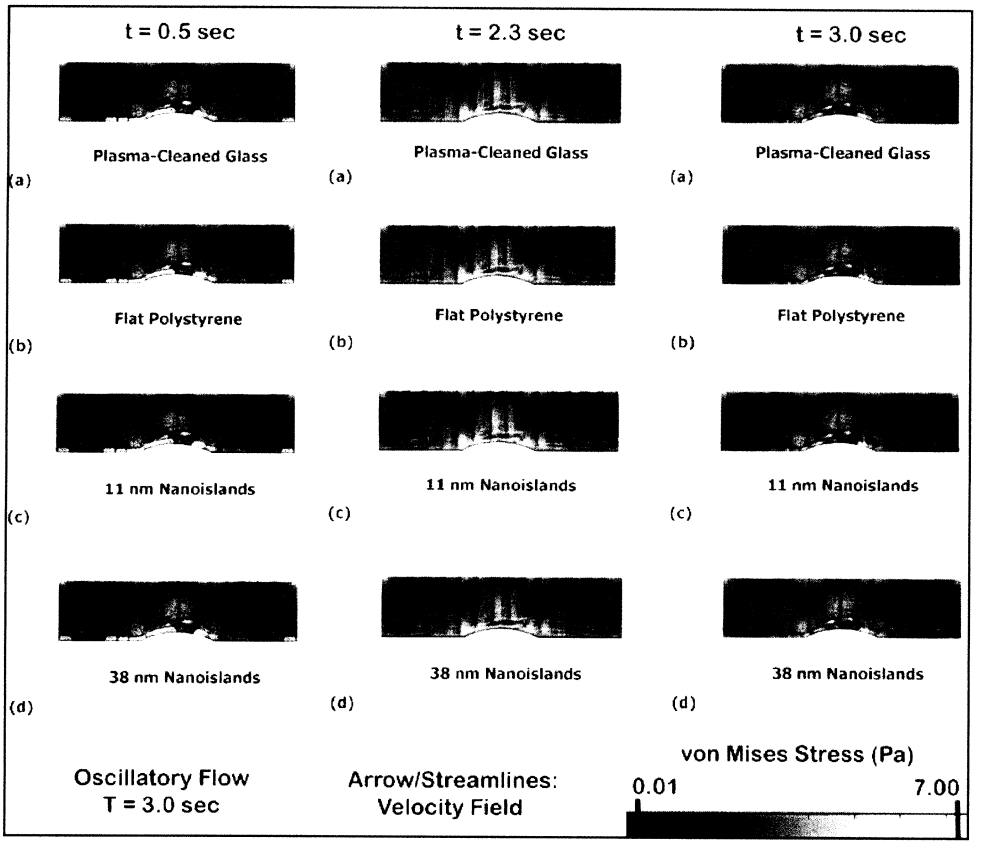

677x583mm (96 x 96 DPI)

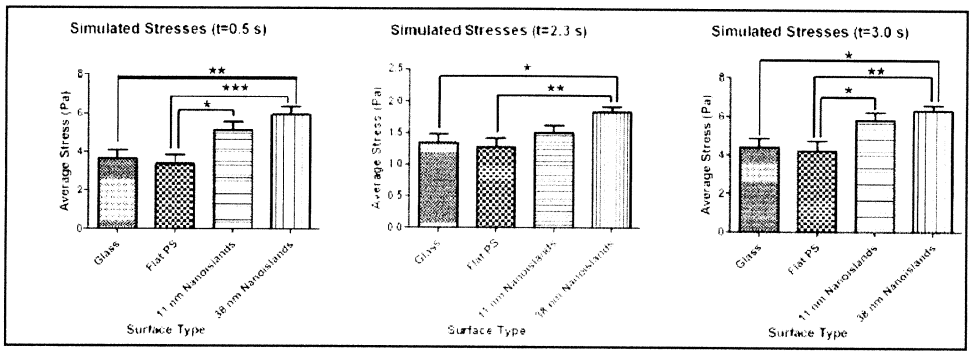

985x347mm (96 x 96 DPI)

Figure 1. FEM Analysis of cell confluence: macroscopic view. Incompressible Navier-Stokes with a Newtonian fluid was assumed.

Figure 2. FEM of cell confluence: microscopic view. (A) 50% confluence with cell at entrance to flow field, (B) 100% confluence with cell at entrance to flow field, (C) 100% confluence with a larger cell height, and (D) 50% confluence without cell at entrance.

Figure 3. Unidirectional fluid flow pattern over a cell with a large cell height.

Figure 4. Shear stresses along the surfaces of cells with varying cell height. Oscillatory fluid flow of media was utilized and these data depict the simulation at t = 3.0 seconds. Red arrows depict the velocity field and the grayscale gradient depicts the von Mises stress distribution in the various simulations.

Figure 5. Shear stresses assessed at the cell center (top), cell left (middle), and cell right (bottom) portion over 3.0 seconds, along with the corresponding averages for each variance.

Figure 6. FEM simulation of oscillatory fluid flow on various substrata at t = 0.5 s, t = 2.3 s, and t =3.0 s. Red arrows depict the velocity field, and the grayscale gradient depicts the von Mises stress distribution in the various simulations.

Figure 7. Average shear stresses in the FEM of oscillatory fluid flow over various substrata at t =0.5 s, t = 2.3 s, and t = 3.0 s. (*: $p < 0.05$, **: $p < 0.01$, ***: $p < 0.001$).

Cell Type	Flow Type	Substrate	Figures	Supplement
Semi-Circular "Bump"	Unidirectional	Flat Polystyrene	1, 2, 3	S.B
1.5 μm High hFOB 3 μm High hFOB 5 μm High hFOB 7 μm High hFOB	Oscillatory	Flat Polystyrene	4, 5	S.A
3 μm High hFOB	Oscillatory	*Plasma-Cleaned Glass *Flat Polystyrene *11 nm Nanoislands *38 nm Nanoislands	6, 7	S.C

Table 1. The varying types of simulations have been summarized here. Preliminary studies used a semi-circular "bump" in unidirectional flow to analyze the effects of confluence on flow patterns. Additionally, these preliminary data were used to examine flow distal to the cell under unidirectional conditions. Varying cell heights of human fetal osteoblastic cells (hFOB) were compared under oscillatory fluid flow conditions to examine the effects of cell height on the relative von Mises stresses imposed upon cells by such flow. Finally, 3 μm high hFOBs were examined under the same oscillatory flow conditions and compared on various substrata. The purpose was to compare the relative von Mises stresses imposed by these flow conditions on cells with varying elastic moduli. All of these analyses and model reports can be found in the figures and supplements noted in the table.

*These substrata were simulated by varying the relative Young's moduli of cells cultured on the various surfaces. Such values were taken from previous experimental data by Hansen et al. (32).

Supplemental Information – COMSOL Model Reports

Contents:

Supplement A – Cell Height Study (S.A)

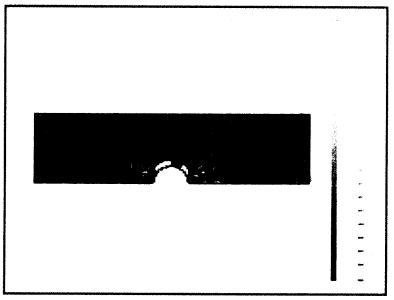

1. Table of Contents

2. Model Properties

Property	Value
Model name	
Author	
Company	
Department	
Reference	
URL	
Saved date	Jun 19, 2008 2:00:43 PM

Creation date	Jun 12, 2008 10:36:24 AM
COMSOL version	COMSOL 3.4.0.248

File name: G:\COMSOL\1.mph

Application modes and modules used in this model:

- Geom1 (2D)
  - Incompressible Navier-Stokes
  - Plane Stress (Structural Mechanics Module)

3. Constants

Name	Expression	Value	Description
w	2*pi[rad/s]		frequency
Patm	0[Pa]		
k	40[Pa/m]		

4. Geometry

4.1. Geom1

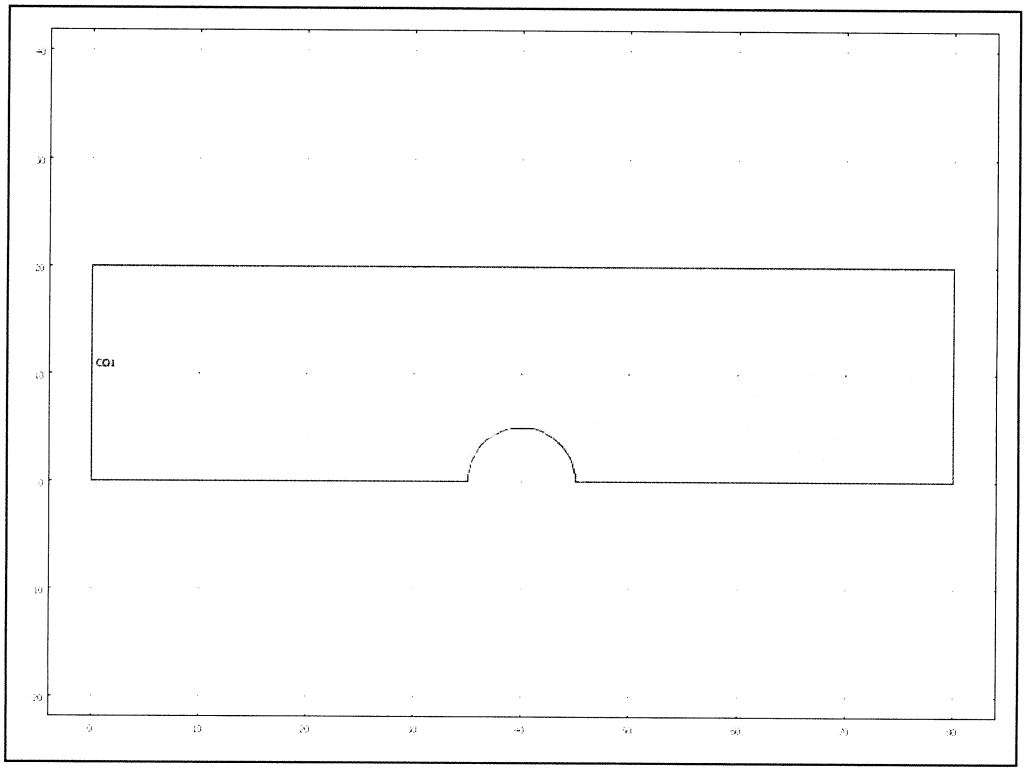

5. Geom1

5.1. Mesh

5.1.1. Mesh Statistics

Number of degrees of freedom	3584
Number of mesh points	224
Number of elements	393
Triangular	393
Quadrilateral	0
Number of boundary elements	53
Number of vertex elements	7
Minimum element quality	0.751
Element area ratio	0.027

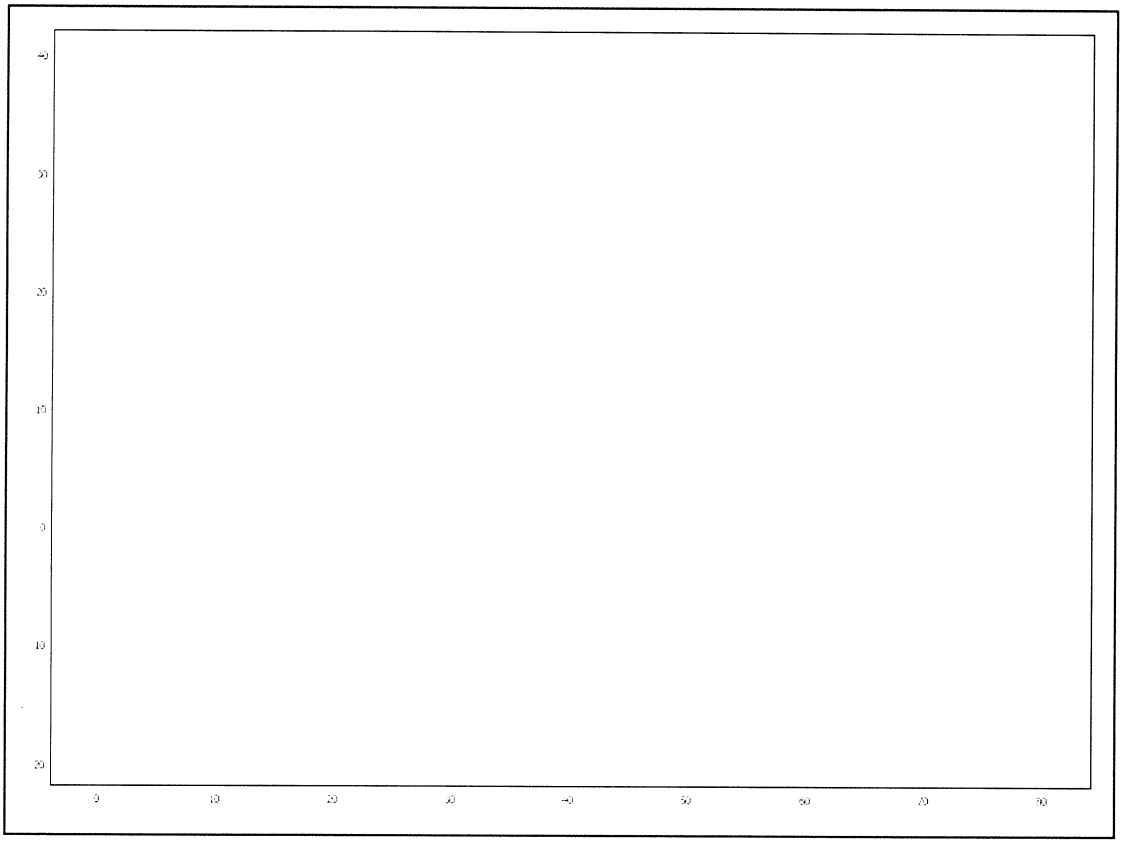

5.2. Application Mode: Incompressible Navier-Stokes (ns)

Application mode type: Incompressible Navier-Stokes

Application mode name: ns

5.2.1. Application Mode Properties

Property	Value
Default element type	Lagrange - P_2 P_1
Analysis type	Transient
Corner smoothing	Off
Frame	Frame (ref)
Weak constraints	Off
Constraint type	Ideal

5.2.2. Variables

Dependent variables: u, v, p, nxw, nyw

Shape functions: shlag(2,'u'), shlag(2,'v'), shlag(1,'p')

Interior boundaries not active

5.2.3. Boundary Settings

Boundary		1	2, 4, 6-7	3
Type		Inlet	Wall	Wall
intype		**p**	uv	uv
walltype		noslip	noslip	**slip**
Pressure (p0)	Pa	**0.5*k*cos(w*t)+Patm**	0	0

Boundary		5
Type		Outlet
intype		uv
walltype		noslip
Pressure (p0)	Pa	**-0.5*k*cos(w*t)+Patm**

5.2.4. Subdomain Settings

Subdomain		1
Integration order (gporder)		**4 4 2**
Constraint order (cporder)		**2 2 1**

5.3. Application Mode: Plane Stress (smps)

Application mode type: Plane Stress (Structural Mechanics Module)

Application mode name: smps

5.3.1. Scalar Variables

Name	Variable	Value	Unit	Description
t_old_ini	t_old_ini_smps	-1	s	Initial condition previous time step (contact with dynamic friction)

5.3.2. Application Mode Properties

Property	**Value**
Default element type	Lagrange - Quadratic
Analysis type	Static
Large deformation	On
Specify eigenvalues using	Eigenfrequency
Create frame	On
Deform frame	Frame (deform)
Frame	Frame (ref)
Weak constraints	Off
Constraint type	Ideal

5.3.3. Variables

Dependent variables: u2, v2, p2

Shape functions: shlag(2,'u2'), shlag(2,'v2')

Interior boundaries not active

5.3.4. Boundary Settings

Boundary		2-4	6-7	1, 5
Follower pressure (P)	Pa	0	**p**	0
loadcond		distr_force	**follower_press**	distr_force
constrcond		free	free	**fixed**

6. Solver Settings

Solve using a script: off

Analysis type	Transient
Auto select solver	On
Solver	Time dependent
Solution form	Automatic
Symmetric	Off
Adaption	Off

6.1. Direct (PARDISO)

Solver type: Linear system solver

Parameter	**Value**
Preordering algorithm	Nested dissection
Row preordering	On
Pivoting perturbation	1.0E-8
Relative tolerance	1.0E-6
Factor in error estimate	400.0
Check tolerances	On

6.2. Time Stepping

Parameter	**Value**
Times	0:0.1:3
Relative tolerance	0.01
Absolute tolerance	0.0010
Times to store in output	Specified times
Time steps taken by solver	Free
Manual tuning of step size	Off
Initial time step	1E-6
Maximum time step	1.0
Maximum BDF order	5
Singular mass matrix	Maybe
Consistent initialization of DAE systems	Backward Euler
Error estimation strategy	Exclude algebraic
Allow complex numbers	Off

Tissue Engineering Part C: Methods
Finite Element Analysis of Fluid Flow Conditions in Cell Culture (doi: 10.1089/ten.TEC.2009.0159)

7. Postprocessing

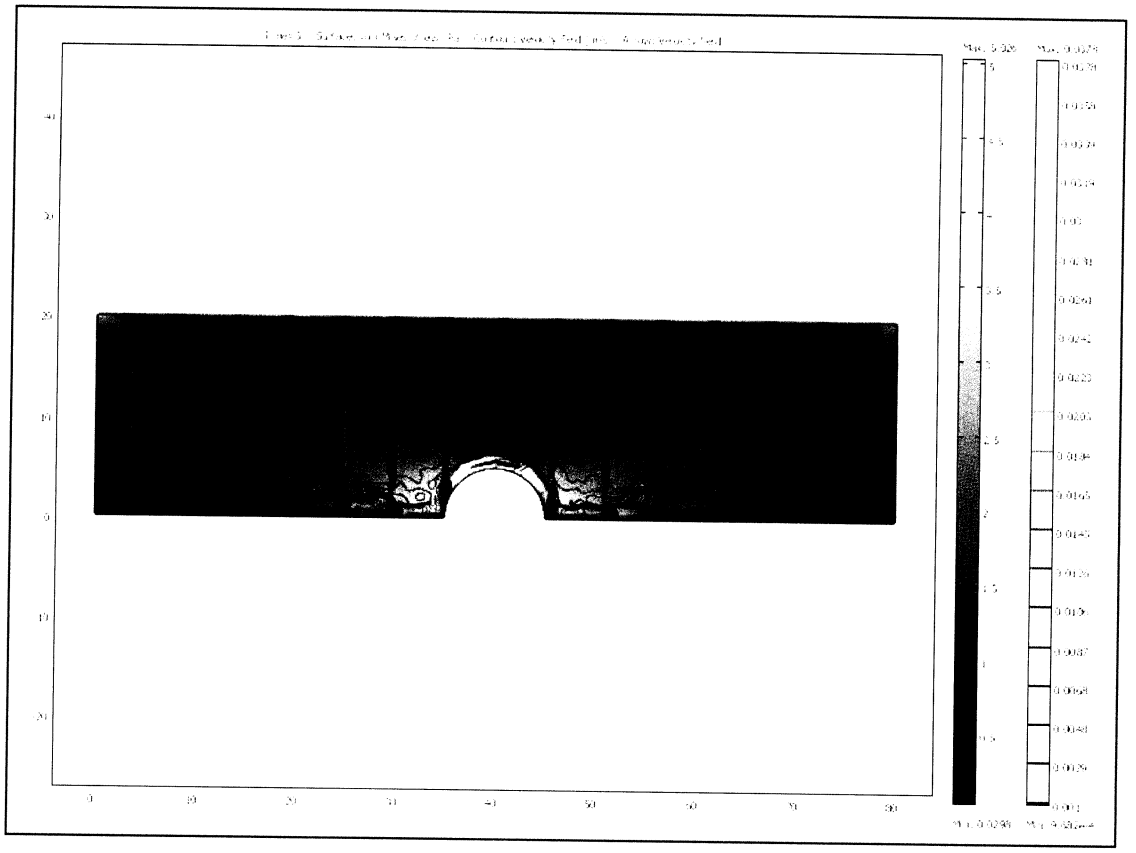

Supplement B – Cell Confluence Study (S.B)

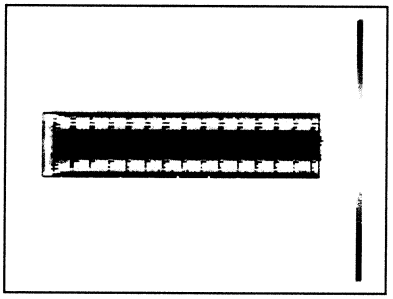

1. Table of Contents

2. Model Properties

Property	Value
Model name	
Author	
Company	
Department	
Reference	
URL	
Saved date	Jun 6, 2008 2:06:39 PM
Creation date	Jun 6, 2008 1:31:37 PM
COMSOL version	COMSOL 3.4.0.248

File name: G:\COMSOL\10%-Confluency.mph

Application modes and modules used in this model:

- Geom1 (2D)
  - Plane Strain (Structural Mechanics Module)
  - Incompressible Navier-Stokes

3. Geometry

Number of geometries: 1

3.1. Geom1

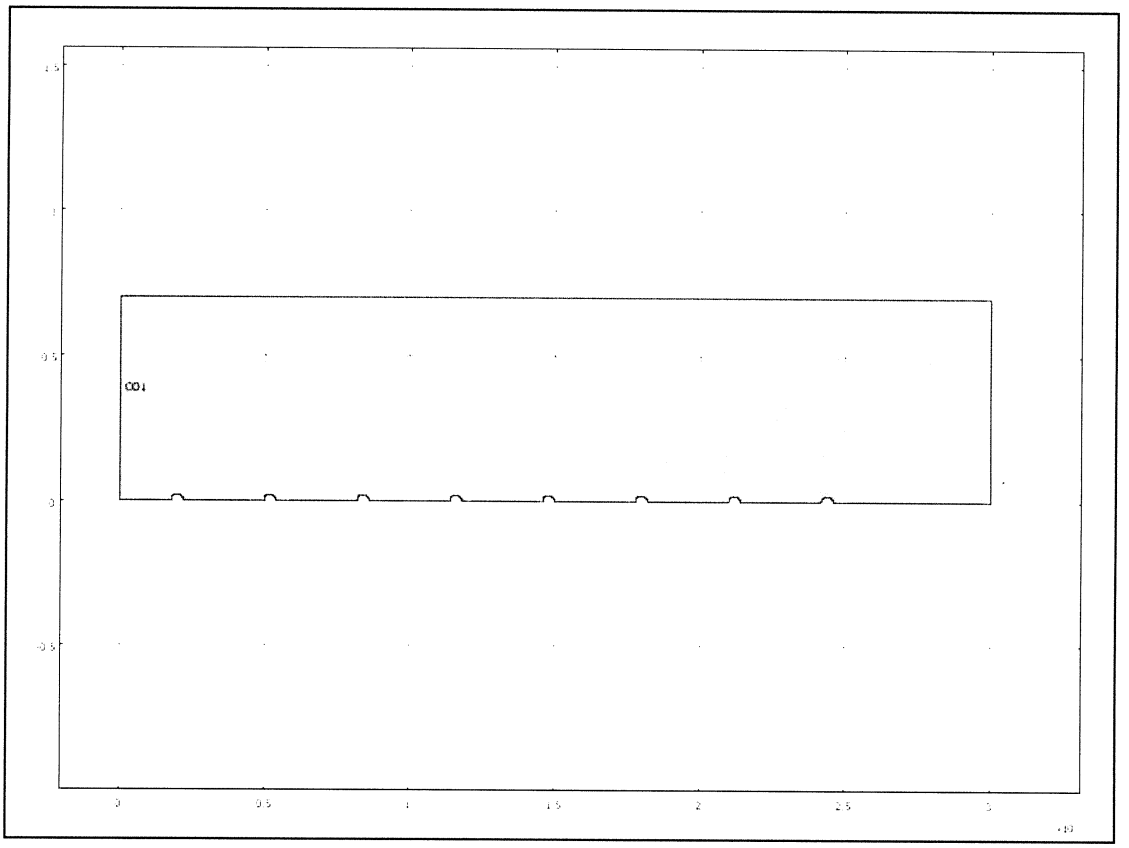

4. Geom1

4.1. Mesh

4.1.1. Mesh Statistics

Number of degrees of freedom	28861
Number of mesh points	1757
Number of elements	3263
Triangular	3263
Quadrilateral	0
Number of boundary elements	249
Number of vertex elements	28
Minimum element quality	0.691
Element area ratio	0

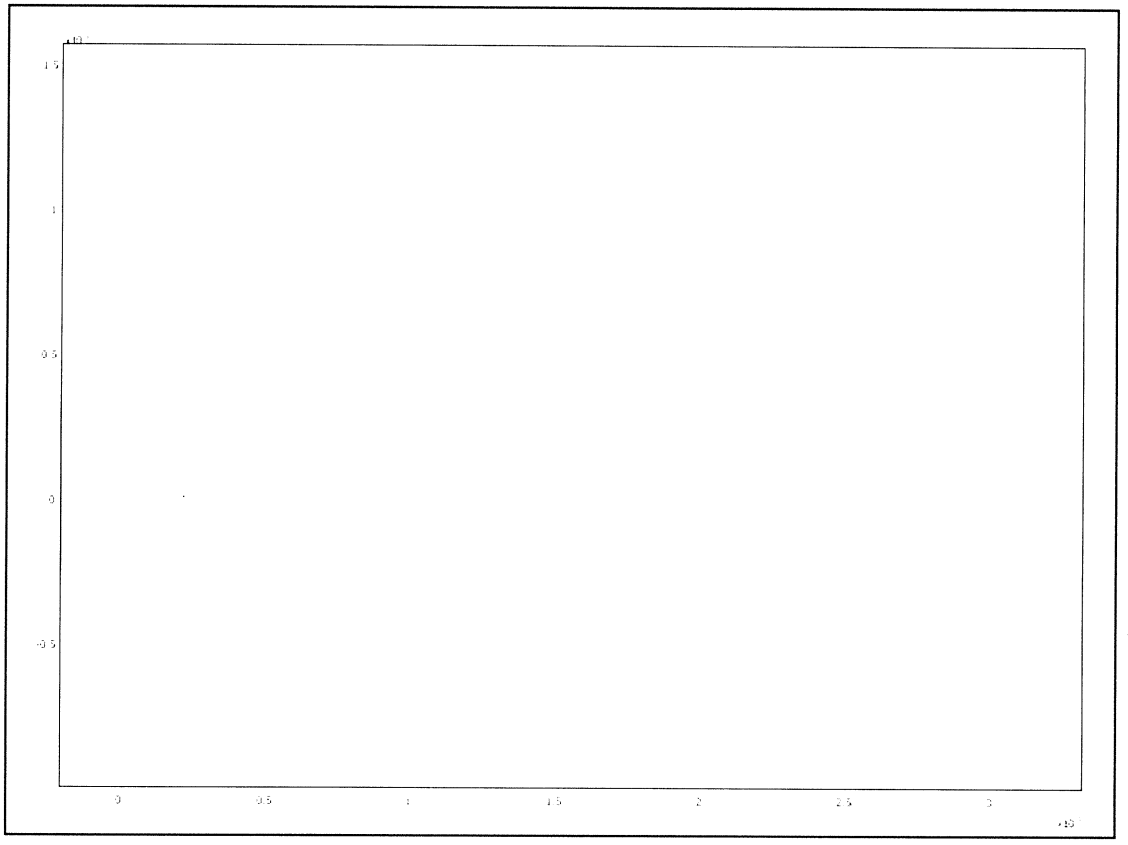

4.2. Application Mode: Plane Strain (smpn)

Application mode type: Plane Strain (Structural Mechanics Module)

Application mode name: smpn

4.2.1. Scalar Variables

Name	Variable	Value	Unit	Description
t_old_ini	t_old_ini_smpn	-1	s	Initial condition previous time step (contact with dynamic friction)

4.2.2. Application Mode Properties

Property	**Value**
Default element type	Lagrange - Quadratic
Analysis type	Static
Large deformation	On
Specify eigenvalues using	Eigenfrequency
Create frame	Off
Deform frame	Frame (ref)
Frame	Frame (ref)
Weak constraints	Off
Constraint type	Ideal

4.2.3. Variables

Dependent variables: u2, v2, p2

Shape functions: shlag(2,'u2'), shlag(2,'v2')

Interior boundaries not active

4.2.4. Subdomain Settings

Subdomain			1
name		**Solid domain**	

4.3. Application Mode: Incompressible Navier-Stokes (ns)

Application mode type: Incompressible Navier-Stokes

Application mode name: ns

4.3.1. Application Mode Properties

Property	Value
Default element type	Lagrange - P_2 P_1
Analysis type	Stationary
Corner smoothing	Off
Frame	Frame (ref)
Weak constraints	Off
Constraint type	Ideal

4.3.2. Variables

Dependent variables: u, v, p, nxw, nyw

Shape functions: shlag(2,'u'), shlag(2,'v'), shlag(1,'p')

Interior boundaries not active

4.3.3. Boundary Settings

Boundary		1	2-11, 13-28	12
Type		Inlet	Wall	Open boundary
Normal inflow velocity (U0in)	m/s	**0.38095238**	1	1

4.3.4. Subdomain Settings

Subdomain		1
Integration order (gporder)		**4 4 2**
Constraint order (cporder)		**2 2 1**

5. Solver Settings

Solve using a script: off

Analysis type	Static
Auto select solver	On
Solver	Stationary
Solution form	Automatic
Symmetric	auto
Adaption	Off

5.1. Direct (PARDISO)

Solver type: Linear system solver

Parameter	Value
Preordering algorithm	Nested dissection
Row preordering	On
Pivoting perturbation	1.0E-8
Relative tolerance	1.0E-6
Factor in error estimate	400.0
Check tolerances	On

5.2. Stationary

Parameter	Value
Linearity	Automatic
Relative tolerance	1.0E-6
Maximum number of iterations	25
Manual tuning of damping parameters	Off
Highly nonlinear problem	On
Initial damping factor	1.0
Minimum damping factor	1.0E-4
Restriction for step size update	10.0

5.3. Advanced

Parameter	Value
Constraint handling method	Elimination

Null-space function	Automatic
Assembly block size	1000
Use Hermitian transpose of constraint matrix and in symmetry detection	Off
Use complex functions with real input	Off
Stop if error due to undefined operation	On
Store solution on file	Off
Type of scaling	None
Manual scaling	
Row equilibration	On
Manual control of reassembly	Off
Load constant	On
Constraint constant	On
Mass constant	On
Damping (mass) constant	On
Jacobian constant	On
Constraint Jacobian constant	On

6. Postprocessing

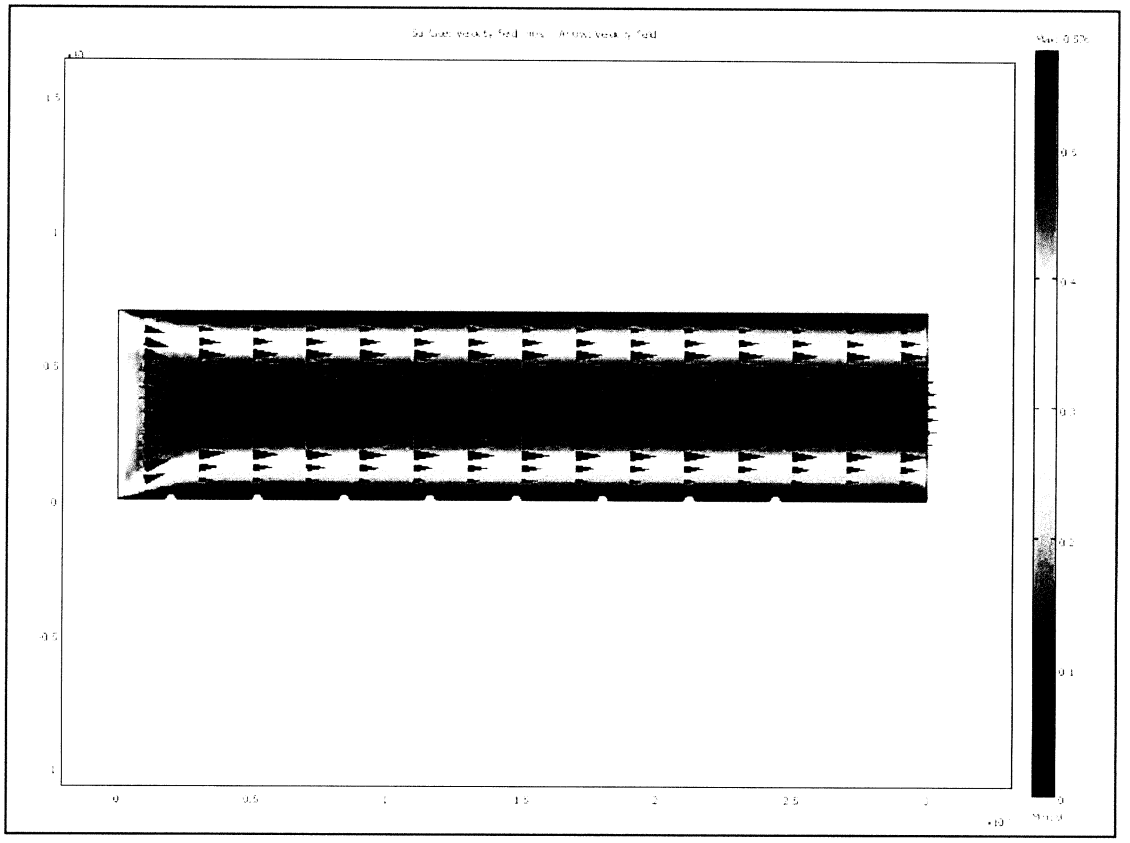

Supplement C – Young's Modulus Study (S.C)

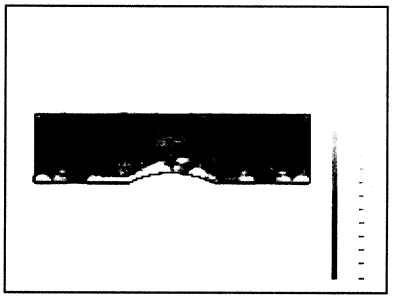

1. Table of Contents

2. Model Properties

Property	Value
Model name	
Author	
Company	
Department	
Reference	
URL	
Saved date	Jul 9, 2008 1:32:46 PM
Creation date	Jun 12, 2008 10:36:24 AM
COMSOL version	COMSOL 3.4.0.248

File name: G:\COMSOL\11 nm.mph

Application modes and modules used in this model:

- Geom1 (2D)
  - Incompressible Navier-Stokes
  - Plane Stress (Structural Mechanics Module)

3. Constants

Name	Expression	Value	Description
w	2*pi[rad/s]		frequency
Patm	0[Pa]		
k	40[Pa/m]		

4. Geometry

Number of geometries: 1

4.1. Geom1

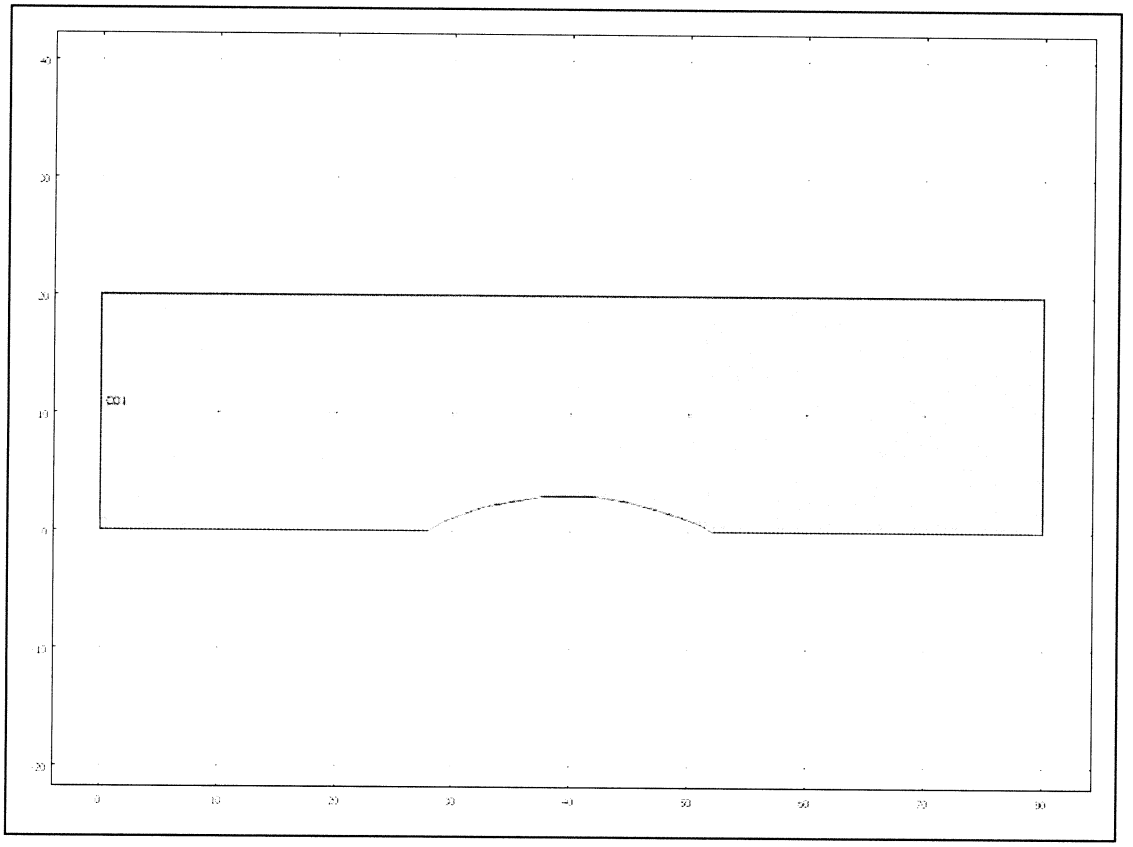

5. Geom1

5.1. Mesh

5.1.1. Mesh Statistics

Number of degrees of freedom	2451
Number of mesh points	155
Number of elements	265
Triangular	265
Quadrilateral	0
Number of boundary elements	43
Number of vertex elements	7
Minimum element quality	0.741
Element area ratio	0.077

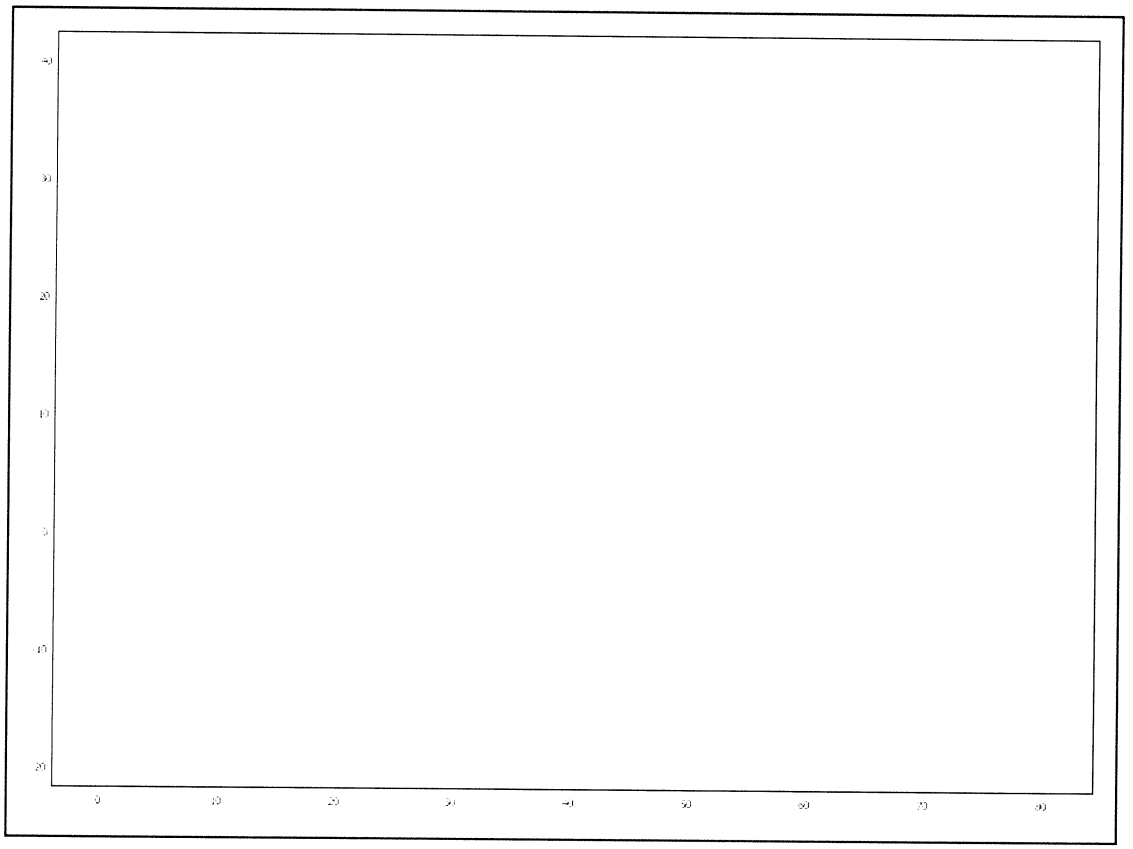

5.2. Application Mode: Incompressible Navier-Stokes (ns)

Application mode type: Incompressible Navier-Stokes

Application mode name: ns

5.2.1. Application Mode Properties

Property	Value
Default element type	Lagrange - P_2 P_1
Analysis type	Transient
Corner smoothing	Off
Frame	Frame (ref)
Weak constraints	Off
Constraint type	Ideal

5.2.2. Variables

Dependent variables: u, v, p, nxw, nyw

Shape functions: shlag(2,'u'), shlag(2,'v'), shlag(1,'p')

Interior boundaries not active

5.2.3. Boundary Settings

Boundary		1	2, 4, 6-7	3
Type		Inlet	Wall	Wall
intype		**p**	uv	uv
walltype		noslip	noslip	**slip**
Pressure (p0)	Pa	**0.5*k*cos(w*t)+Patm**	0	0

Boundary		5
Type		Outlet
intype		uv
walltype		noslip
Pressure (p0)	Pa	**-0.5*k*cos(w*t)+Patm**

5.2.4. Subdomain Settings

Subdomain		1
Integration order (gporder)		**4 4 2**
Constraint order (cporder)		**2 2 1**

5.3. Application Mode: Plane Stress (smps)

Application mode type: Plane Stress (Structural Mechanics Module)

Application mode name: smps

5.3.1. Scalar Variables

Name	Variable	Value	Unit	Description
t_old_ini	t_old_ini_smps	-1	s	Initial condition previous time step (contact with dynamic friction)

5.3.2. Application Mode Properties

Property	**Value**
Default element type	Lagrange - Quadratic
Analysis type	Static
Large deformation	On
Specify eigenvalues using	Eigenfrequency
Create frame	On
Deform frame	Frame (deform)
Frame	Frame (ref)
Weak constraints	Off
Constraint type	Ideal

5.3.3. Variables

Dependent variables: u2, v2, p2

Shape functions: shlag(2,'u2'), shlag(2,'v2')

Interior boundaries not active

5.3.4. Boundary Settings

Boundary		2-4	6-7	1, 5
Follower pressure (P)	Pa	0	**p**	0
loadcond		distr_force	**follower_press**	distr_force
constrcond		free	free	**fixed**

5.3.5. Subdomain Settings

Subdomain		1
Young's modulus (E)	Pa	**9000**

6. Solver Settings

Solve using a script: off

Analysis type	Transient
Auto select solver	On
Solver	Time dependent
Solution form	Automatic
Symmetric	Off
Adaption	Off

6.1. Direct (PARDISO)

Solver type: Linear system solver

Parameter	**Value**
Preordering algorithm	Nested dissection
Row preordering	On
Pivoting perturbation	1.0E-8
Relative tolerance	1.0E-6
Factor in error estimate	400.0
Check tolerances	On

6.2. Time Stepping

Parameter	**Value**
Times	0:0.1:3
Relative tolerance	0.01
Absolute tolerance	0.0010
Times to store in output	Specified times
Time steps taken by solver	Free
Manual tuning of step size	Off
Initial time step	1E-6
Maximum time step	1.0
Maximum BDF order	5
Singular mass matrix	Maybe
Consistent initialization of DAE systems	Backward Euler

6.3. Advanced

Parameter	Value
Constraint handling method	Elimination
Null-space function	Automatic
Assembly block size	1000
Stop if error due to undefined operation	On
Store solution on file	Off
Type of scaling	Automatic
Row equilibration	On
Load constant	On
Constraint constant	On
Mass constant	On
Damping (mass) constant	On
Jacobian constant	On
Constraint Jacobian constant	On

7. Postprocessing